IRIS AperTO

UNIVERSITÀ DEGLI STUDI DI TORINO

AperTO - Archivio Istituzionale Open Access dell'Università di Torino

A molecularly annotated model of patient-derived colon cancer stem-like cells to assess genetic and non-genetic mechanisms of resistance to anti-EGFR therapy

This is the author's manuscript

Original Citation:

Availability:

This version is available http://hdl.handle.net/2318/1662775 since 2018-03-20T09:28:51Z

Published version:

DOI:10.1158/1078-0432.CCR-17-2151

Terms of use:

Open Access

Anyone can freely access the full text of works made available as "Open Access". Works made available under a Creative Commons license can be used according to the terms and conditions of said license. Use of all other works requires consent of the right holder (author or publisher) if not exempted from copyright protection by the applicable law.

(Article begins on next page)

17 April 2024

A molecularly annotated model of patient-derived colon cancer stem-like cells to assess genetic and non-genetic mechanisms of resistance to anti-EGFR therapy.

Paolo Luraghi[1], Viola Bigatto[1], Elia Cipriano[1,2], Gigliola Reato[1,2], Francesca Orzan[1], Francesco Sassi[1], Francesca De Bacco[1], Claudio Isella[1], Sara E. Bellomo[1], Enzo Medico[1,2], Paolo M. Comoglio[1], Andrea Bertotti[1,2], Livio Trusolino[1,2], and Carla Boccaccio[1,2,3].

[1]Candiolo Cancer Institute, FPO-IRCCS, Str. Prov. 142, 10060 Candiolo, Torino, Italy
[2]Department of Oncology, University of Torino, 10060 Candiolo, Torino, Italy

Running title: colon cancer stem-like cells and EGFR therapy resistance

Keywords: colorectal cancer, cancer stem-like, EGFR, ERBB3, targeted therapy

Grant Support: This work was supported by AIRC, Italian Association for Cancer Research ("Special Program Molecular Clinical Oncology 5xMille, N. 9970"; IG 15709 to C.B., 15572 to P.M.C., 18532 to L.T., 15571 to A.B.), Transcan (L.T.), TACTIC (L.T.), Fondazione Piemontese per la Ricerca sul Cancro-ONLUS, 5x1000 Ministry of Health (L.T.) and Italian Ministry of Health (Ricerca Corrente).

[3]**Corresponding author**:
Carla Boccaccio
Candiolo Cancer Institute, FPO-IRCCS, Str. Prov. 142,10060 Candiolo, Torino, Italy
phone: +39-011-9933208; fax: +39-011-9933225; e-mail: carla.boccaccio@ircc.it.

Translational relevance

Reliable pre-clinical models are needed to speed-up the clinical development of new effective cancer therapies. A large collection of metastatic colorectal cancer xenopatients has been successfully exploited to identify new genetic mechanisms of resistance to the anti-EGFR antibody cetuximab and to prove the efficacy of new treatment strategies. From xenopatients, we derived an ample collection of stem-like cultures (xenospheres), faithfully mirroring the genetic, biological and pharmacological properties of xenopatients. Xenospheres offered the unique opportunity to study *in vitro* and *in vivo* non-genetic mechanisms of resistance that can be underestimated in xenopatients. Through this approach, we provide robust preclinical evidence that NRG1 is a crucial biomarker to predict both cetuximab resistance in the absence of genetic mechanisms, and response to pan-HER inhibition. Xenospheres are thus a reliable patient-derived *in vitro* model, required to complement xenopatients in elucidating the mechanisms of response to targeted therapies in metastatic colorectal cancer.

Abstract

Purpose Patient-derived xenografts ("*xenopatients*") of colorectal cancer metastases have been essential to identify genetic determinants of resistance to the anti-EGF Receptor (EGFR) antibody cetuximab, and to explore new therapeutic strategies. From xenopatients, a genetically annotated collection of stem-like cultures ("*xenospheres*") was generated and characterized for response to targeted therapies.

Experimental Design. Xenospheres underwent exome-sequencing analysis, gene expression profile and *in vitro* targeted treatments to assess genetic, biological and pharmacological correspondence with xenopatients, and to investigate non-genetic biomarkers of therapeutic resistance. The outcome of EGFR family inhibition was tested in an *NRG1*-expressing *in vivo* model.

Results. Xenospheres faithfully retained the genetic make-up of their matched xenopatients over *in vitro* and *in vivo* passages. Frequent and rare genetic lesions triggering primary resistance to cetuximab through constitutive activation of the RAS signaling pathway were conserved, as well as the vulnerability to their respective targeted treatments. Xenospheres lacking such alterations (RAS^{wt}) were highly sensitive to cetuximab, but were protected by ligands activating the EGFR family, mostly NRG1. Upon reconstitution of *NRG1* expression, xenospheres displayed increased tumorigenic potential *in vivo*, generated tumors completely resistant to cetuximab, and sensitive only to comprehensive EGFR family inhibition.

Conclusions. Xenospheres are a reliable model to identify both genetic and non-genetic mechanisms of response and resistance to targeted therapies in colorectal cancer. In the absence of RAS pathway mutations, NRG1 and other EGFR ligands can play a major role in conferring primary cetuximab resistance, indicating that comprehensive inhibition of the EGFR family is required to achieve a significant therapeutic response.

Introduction

In metastatic colorectal cancer (mCRC), monoclonal antibodies against the Epidermal Growth Factor Receptor (EGFR), associated with standard chemotherapies, significantly extended the median overall survival (from 20 to 30 months) in a fraction of patients (1). In the vast majority of such responsive cases, EGFR inhibition is effective in the absence of any genetic alteration of the receptor (2,3). This exception to the "oncogene addiction" rule can be explained by the critical role that normal EGFR, physiologically stimulated by its ligand(s), plays in supporting colorectal cancer cell proliferation. This role is likely rooted in the cancer stem-like subpopulation, which, like its normal stem/progenitor counterpart, exquisitely depends on EGF signaling (4,5). In mCRC patients refractory to EGFR inhibition, the tumor often harbors genetic alterations such as *KRAS* or *BRAF* mutations, hijacking the control of the proliferative pathway downstream EGFR (6). Recently, new less frequent genetic mechanisms of resistance were identified, thanks to the analysis of a large collection of xenopatients. These mechanisms include *ERBB2/MET* amplifications (7,8), *ERBB2* mutations (9), *IGF2* overexpression (10) and *EGFR* mutations (11,12). Such alterations represent actionable therapeutic targets, and, indeed, patients with *ERBB2* amplification underwent a successful clinical trial (13).

Interestingly, as shown by whole exome genetic analysis of an ample panel of xenopatients, in a fraction of refractory cases a genetic mechanism of resistance to EGFR inhibition has not been identified (11). In such cases, as suggested by previous studies (10,14) complete or partial resistance to cetuximab can be explained by the presence of autocrine or paracrine circuits of growth factors. Ligands of the EGF family, which fall in two main groups based on their ability to directly bind EGFR or another member of the EGFR family (15,16), can provide such a mechanism of resistance, as they could either compete or bypass cetuximab inhibition (17,18). For studying the outcome of paracrine signals, xenopatients may suffer from limitations, mainly because relevant growth factors can be underrepresented in the tumor microenvironment, or the murine ligands can fail to cross-react with human receptors. In a proof-of-concept study, we recently showed that xenopatient-derived cultures of stem-like cells (xenospheres) are a valuable system to address these issues *in vitro* and *in vivo* (5).

Xenospheres provide a unique counterpart of the original tumor and xenopatient, as they are amenable to *in vitro* quantitative measurement of proliferative responses, and, *in vivo*, they can regenerate phenocopies of the original tumor to provide a meaningful preclinical model (5,19). In this study we derived an ample collection of xenospheres and showed that

they retain a remarkable genetic, biological and pharmacological correspondence with original mCRC xenopatients. In xenospheres lacking oncogenic activation of the RAS pathway, we could identify NRG1 as the main EGF family ligand able to substitute EGF in sustaining proliferation, and to induce primary resistance to cetuximab by engaging ERBB3. We could then show that broad inhibition of the EGFR family is more effective than selective inhibition of EGFR alone.

METHODS

Xenosphere generation and genetic characterization

All procedures involving animal experimentation were approved by the Italian Ministry of Health and by the internal Ethical Committee for Animal Experimentation. Xenospheres were derived as previously described (5). Genomic DNA was extracted with the Wizard® SV genomic DNA purification system (Promega) and analyzed for *KRAS, NRAS, BRAF, PIK3CA* mutations as previously described (8). Whole exome sequencing analysis was performed by PGD (Personal Genome Diagnostics) as previously described for the corresponding xenopatients, using the same settings and specific controls (11). Data concerning gene mutations and copy number variations (CNV) were extracted and analyzed. CNV include complete gene deletions and copy gains >4.

Cell viability assay

Cells were plated at clonal density (10 cells/µl) in ultra-low attachment 96-well plates (Corning-Sigma) in basal stem-cell medium (i.e. with 0,4 ng/ml of EGF). 20 ng/ml of Growth factors (EGF, bFGF, HGF, TGFα, HBEGF, EREG, AREG, NRG1, Peprotech) and inhibitors (10 µg/ml cetuximab, 10 µg/ml Panitumumab, 0,5 µM Gefitinib, 0,5 µM Lapatinib, 2µM PLX-4720) were added at day 0. ATP production was measured using Cell Titer Glo® (Promega) and GloMax 96 MicroplateLuminometer (Promega).

Western blot

Immunoblottings were analyzed with the following antibodies: rabbit anti-phospho EGFR (Tyr1068, Cell Signaling Technology), rabbit monoclonal anti-EGFR (Cell Signaling Technology), mouse monoclonal anti-ERBB2 (Santa Cruz Biotechnolgy), rabbit anti-phospho ERBB3 (Tyr1289 Cell Signaling Technology), rabbit monoclonal anti-ERBB3 (Cell signaling Technology), rabbit anti-phospho ERK 1/2 (Thr202/Tyr204, Cell Signaling Technology), rabbit anti-ERK 1/2, rabbit anti-phospho AKT (Ser473, Cell Signaling Technology), rabbit anti-AKT (Cell Signaling Technology), rabbit anti-phospho S6 (Ser235/236, Cell Signaling Technology), rabbit anti-S6 (Cell Signaling Technology). Mouse monoclonal anti-vinculin (Sigma Aldrich) antibody was used as control of equal protein loading.

Flow-cytometric analysis

Immunophenotype was performed by incubating $2x10^5$ cells with appropriate dilutions of the following antibodies: anti-EGFR-PE (BD Biosciences) anti-ERBB3-APC (BioLegend). DAPI

was added for dead cell exclusion. Samples were analyzed in a CyAN ADP (DakoCytomation). Data were processed using Summit 4.3 software (DakoCytomation).

Generation of NRG1-expressing xenospheres

$KRAS^{wt}$-Ctx-S xenospheres (CRC0059 and CRC0078) were stably transduced with a human NRG1-expressing lentiviral vector (Origene). *NRG1* RNA expression was evaluated *in vitro* by qPCR using TaqMan® gene expression probe Hs00247620_m1 on ABI PRISM 7900HT sequence detection system according to manufacturer instructions. Ubiquitin (Hs00824723_m1) and beta-actin (Hs99999903_m1) were used as housekeeper genes. *In vivo* NRG1 RNA expression was evaluated by RNA-ISH using RNAscope® technology (Advanced Cell Diagnostic, Inc.) according to manufacturer instructions.

Spheropatient generation and therapy

Dissociated xenospheres ($5x10^4$ cells) were resuspended in a 1:1 mixture of stem-cell medium and matrigel (BD Bioscience), and subcutaneously injected into NOD/SCID male mice (Charles River Laboratories). When tumors reached an average volume of 400 mm^3, mice were randomized and treated with 20 mg/kg cetuximab (Merck) twice-weekly by IP injection, and/or with 150 mg/kg of lapatinib (Hospital Pharmacy), or 40 mg/kg of neratinib (Selleckchem), or 20 mg/kg of afatinib (Sequoia Research Products) by daily oral gavage. Tumor size was measured once-weekly by caliper, and volume was calculated using the formula $(4/3\pi d/2)^2 D/2$, where d is the minor and D is the major tumor axis.

Immunohistochemistry

Tumor sections were formalin-fixed, paraffin-embedded, processed according to standard procedures, and analyzed with the following antibodies: anti-phospho-S6 rabbit monoclonal (Ser235/236, Cell Signaling Technology) and anti-phospho-ERK1/2 rabbit monoclonal (Thr202/204; Cell Signaling Technology).

Statistical analysis

Results were expressed as means ± standard error of the mean (SEM). Statistical significance was evaluated by one-way ANOVA followed by Bonferroni's Multiple Comparison Test, using GraphPad Prism software. $p<0.05$ was considered statistically significant.

For more detailed methods see Supplementary Experimental Procedures

RESULTS

Derivation of a molecularly annotated xenosphere biobank

From mCRC xenopatients (8), we previously derived and characterized a small panel of "xenospheres" (5). These were shown to fulfill the requirements of colon cancer stem-like cells as, (i) *in vitro*, they retained self-renewal and pseudo-differentiative ability, and (ii) upon injection into immunocompromised mice, they formed tumors ("spheropatients") that reproduced both the same histological features and therapeutic response to cetuximab as the original tumors (Fig. 1A) (5).

We now expanded our collection to obtain xenospheres from 58 different xenopatients (8-11,20,21), which were molecularly annotated for the presence of somatic mutations in *KRAS*, *NRAS*, *PIK3CA*, and *BRAF* genes (Fig. 1B, Supplementary Table-S1), known to predict primary resistance to anti-EGFR therapy in patients and xenopatients (8). The frequency of *KRAS* mutations in xenospheres (35%) was similar to that found in both patients and xenopatients (8,22), suggesting lack of *in vitro* selection. Xenospheres without mutations in any of the above 4 genes ("quadruple wild-type", n = 32/58) could be further grouped according to the presence or absence of biomarkers recently associated with resistance to cetuximab in xenopatients, such as *IGF2* overexpression (10), *EGFR* mutations in the extracellular domain (11,12), *ERBB2* amplification or mutations (8,9), or *PTEN* deletion (11) (Fig. 1B). Notably, 18/32 of these xenospheres (WT) were devoid of any of the above alterations.

The gene expression profiles of 28 randomly chosen matched xenospheres and xenopatients were compared to investigate the biological correspondence between the two models, showing a high level of overlapping between the transcriptome of matched samples (Fig. 1C and Supplementary Table-S2). Overall, these findings show that *in vitro* cultured colon cancer stem-like cells maintain both genetic and biological features of the tumor of origin.

Xenospheres faithfully retain the whole genetic make-up of xenopatients

In order to investigate whether xenospheres faithfully retain also the whole genetic make-up of xenopatients, 10 xenospheres derived from xenopatients that had undergone whole exome sequencing (WES) were analyzed using the same technological platform (Fig. 2A and Supplementary Tables S3,S4) (11). As the xenopatient WES was performed to identify new genetic biomarkers of anti-EGFR therapy resistance, all the cases were $KRAS^{wt}$ (11). In xenospheres, the total number of copy number variations (CNV) ranged from 0 to 58 (with an

average of 16, against 22 in the corresponding xenopatients), while somatic mutations ranged from 93 to 244 (with an average of 148, against 129 in xenopatients) (Supplementary Table-S5). The majority of CNV and somatic mutations were shared between xenospheres and matched xenopatients (Fig. 2B,C), with only few exceptions: CNV in CRC0574 (Fig. 2B), and somatic mutations in CRC0078 and CRC0254 (Fig. 2C). Shared lesions included also recently identified biomarkers of resistance to cetuximab such as *ERBB2* amplification (CRC0080), *ERBB2* mutation (CRC0151), $EGFR^{ecd}$ mutation (CRC0104) and $PTEN^{del}$ (CRC0394) (Supplementary Table-S1) (8-12).

Interestingly, the somatic mutations shared between xenospheres and the matched xenopatients displayed an average allelic frequency of ~50%, while lesions private to either model displayed a frequency of ~30% (Fig. 2D). This is in accordance with the notion that genetic alterations required for the oncogenic phenotype ("driver" lesions), should be both shared within the same cell population (high allelic frequency) and conserved during the passage from tumor tissue to xenosphere culture. These features are consistent with the neutral tumor evolution model, recently proposed also for colorectal cancer (23,24).

Moreover, somatic mutations common to xenospheres and xenopatients displayed highly similar allelic frequencies in the two models, further attesting that xenospheres faithfully retain the genetic make-up of xenopatients (Fig. 2E). Exceptions were CRC0078 xenospheres, which displayed a lower grade of correspondence with the original xenopatient, both in the number of shared somatic mutations and their allelic frequency correlation (Fig. 2C,E). This could be explained by two mechanisms: (i) *in vitro* selection of a pre-existing xenopatient subclone (due to sample bias or to selection during cell culture) and/or (ii) xenosphere genetic drift occurred during multiple *in vitro* passages. To identify the underlying mechanism, WES analysis of CRC0078 xenospheres was longitudinally compared with that of two further *in vitro* derivatives of the same lineage: (i) a secondary CRC0078 xenosphere ($CRC0078^{2nd}$), derived from the spheropatient, and previously shown to retain the same biological and tumorigenic properties of the primary xenosphere (5), and (ii) a primary cell culture selected in adherent standard cell culture conditions from the secondary xenosphere ($CRC0078^{ad}$) (Fig. 3A). While the total number of CNV was conserved in the three *in vitro* models (Fig. 3B), a progressive increase of somatic mutations was observed in $CRC0078^{2nd}$ and $CRC0078^{ad}$ (Fig. 3C). As the number of mutations shared between each model with the original xenopatient remained constant, this increase indicated accumulation of new private lesions. Notably, the average allelic frequency of such lesions was lower, as compared with the frequency of lesions shared with the original xenopatient (Fig. 3D), as

observed in all other xenospheres (Fig. 2D). Moreover, the allelic frequencies of single genes shared between each *in vitro* model and the xenopatient (Fig. 3E), or between the different *in vitro* models (Fig. 3F), were highly conserved. These data suggest that CRC0078 xenospheres likely derive from a pre-existing xenopatient subclone, and can accumulate new mutations that, however, for their low allelic frequency, are supposed to be mainly passengers.

Collectively, WES analyses indicate that xenospheres qualitatively and quantitatively reproduce, and stably retain over multiple *in vitro* passages, the landscape of relevant genetic alterations of the original tumors.

The cetuximab response of xenospheres correlates with genetic and non-genetic biomarkers of resistance.

Having shown that xenospheres faithfully retain both biological and genetic features of xenopatients, we assessed the response of xenospheres to anti-EGFR therapy with cetuximab, and its correlation with the presence of genetic determinants of resistance. The response was assessed in a panel of 46 xenospheres, using previously described cell culture conditions (5). As observed in xenopatients (8,11), cetuximab-resistant xenospheres mostly harbored *KRAS* mutations, while most of cetuximab-sensitive xenospheres were quadruple WT (Fig. 4A). Interestingly, among xenospheres lacking *KRAS* mutations ($KRAS^{wt}$) we could discriminate two subgroups (Fig. 4B): those derived from xenopatients that displayed cetuximab resistance (Ctx-R), and those derived from xenopatients that displayed cetuximab sensitivity (Ctx-S), which included tumors that either underwent shrinkage or stabilization (8,10,11,21). Interestingly, $KRAS^{wt}$-Ctx-R xenospheres were enriched with cases harboring genetic alterations activating the RAS pathway (Fig. 4B). These lesions were recently described to be negative predictors of response to anti-EGFR therapy, and were exploited as new targets to overcome resistance in xenopatients (8-11). Coherently, we observed similar correspondences in xenospheres (Fig. 4C): those harboring somatic mutations in the *EGFR* extracellular domain (CRC0104) and in *ERBB2* (CRC0151) were resistant to cetuximab but sensitive to EGFR/ERBB2 small molecule kinase inhibitors; *BRAF* mutated xenospheres (CRC0480) were resistant to cetuximab but sensitive to BRAF inhibition, and were partially protected by EGF, consistently with the notion that EGFR activation protect against BRAF inhibition in CRC (Fig. 4C) (25).

According to the presence of these oncogenic drivers, $KRAS^{wt}$-Ctx-R xenospheres were fully independent of exogenous EGF for their proliferation, similarly to $KRAS^{mut}$ xenospheres (Supplementary Fig. 1A). *Vice-versa*, the $KRAS^{wt}$-Ctx-S subgroup mainly

included xenospheres that lacked mutations known to activate the RAS pathway (Fig. 4B), and was strongly dependent on exogenous EGF for their proliferation (Supplementary Fig. 1A). This indicates that these xenospheres lack a cell-autonomous genetic driver of proliferation. Therefore they represent cases that, on the one hand, are susceptible to EGFR inhibition, and, on the other hand, can be affected by growth factors that can protect against different kinase inhibitors (26,27). Remarkably, the latter could be underestimated in conventional xenopatients, as we showed for HGF (5).

Therefore, we set out to systematically investigate which signals could confer to $KRAS^{wt}$ xenospheres the ability to circumvent the proliferative block imposed by EGFR inhibition with cetuximab. $KRAS^{wt}$ xenospheres were kept in the presence of growth factors that activate the EGFR family (the EGFR ligands EGF, TGFα, HBEGF, EREG, AREG and the ERBB3 ligand NRG1), and other tyrosine kinase receptors (bFGF and HGF). The response to cetuximab, measured as cell viability, was compared to that of untreated cells (Fig. 4D,E and Supplementary Fig. S1B). As expected, viability of the $KRAS^{wt}$-Ctx-R xenosphere group kept in basal medium was overall poorly affected by cetuximab, and poorly modulated in the presence of the other growth factors (Fig. 4D). In contrast, the viability of the $KRAS^{wt}$-Ctx-S xenosphere group was strongly impaired by cetuximab in basal medium, but it was at least in part preserved in the presence of other growth factors (Fig. 4E). These showed different abilities to protect from cetuximab: (i) negligible for EREG and AREG (viability < 0.4); (ii) intermediate for TGFα, HBEGF, HGF and bFGF (0.4 < viability < 0.8); (iii) maximum for EGF and NRG1 (viability > 0.8).

Taken together, these data indicate that xenospheres reproduce the correspondence observed in xenopatients between the genetic make-up on the one hand, and the therapeutic response to cetuximab or other targeted drugs on the other. Moreover, xenospheres lacking any known genetic determinants of resistance retain cetuximab sensitivity and can be exploited to qualitatively and quantitatively measure the ability of growth factors to compensate for EGFR inhibition.

EGF family ligands differently modulate EGFR activity and cetuximab response

In order to investigate the mechanisms of cetuximab primary resistance conferred by exogenous growth factors, we focused on the EGF family of ligands, whose expression in patients has been correlated with the cetuximab response (28-30). First, expression of EGFR family members ERBB1/2/3 (not ERBB4, undetectable in gene expression profiling) was assessed in western blots of xenospheres kept in basal medium (Supplementary Fig. S2A).

EGFR and ERBB3 proteins were expressed by most xenospheres, with the exception of one single case (CRC0729) that did not express EGFR and was completely insensitive to any of its ligands (Supplementary Fig. S2A,B). ERBB2 was significantly detectable in only two cases (CRC0394 and CRC0080), one of which (CRC0080) was ERBB2-amplified (Supplementary Fig. S2A).

Next we investigated whether the different ability of EGF family ligands to sustain cetuximab resistance (as shown in Fig. 4E) was associated with ligand-specific mechanisms of EGFR family activation. EGF-like ligands such as EGF, TGFα, HBEGF, AREG, and EREG, that bind EGFR (15), can directly outcompete the antibody, while NRG1, which binds ERBB3 and induces formation of heterodimers with either EGFR or ERBB2, is likely to bypass EGFR inhibition by cetuximab (Supplementary Fig. S3A). $KRAS^{wt}$-Ctx-S xenospheres were kept in the presence of each ligand and biochemically analyzed. All EGF-like ligands activated ERK and AKT to a similar extent, while NRG1 hyperactivated both (Fig. 5A). The respective ability of EGF-like ligands to protect from cetuximab was correlated with a different ability to modulate EGFR total protein levels (Fig. 5A) and cell-surface expression (Fig. 5B): indeed, EGF (maximum protection against cetuximab) induced complete EGFR internalization and degradation, while TGFα and HBEGF (intermediate protection) showed only a partial effect on EGFR, and EREG and AREG (negligible protection) did not induce any EGFR internalization and degradation (Fig. 5A,B). As expected, NRG1 did not cause EGFR internalization, which mostly requires EGFR homodimerization (31,32). Interestingly, the EGF ability to induce EGFR internalization is inversely proportional to its concentration, and becomes negligible at doses that induce cell proliferation but are fully inhibited by cetuximab (Supplementary Fig. S3B,C). We can thus hypothesize that EGF-like ligands (or ligand concentrations) that do not induce efficient EGFR downregulation from the cell surface leave the receptor exposed to the competing activity of cetuximab, while those that induce internalization provide an escape from cetuximab and a site of intracellular signaling.

NRG1 sustains xenosphere resistance to cetuximab but full sensitivity to lapatinib

The above findings highlighted that NRG1 can powerfully activate EGFR signaling - the essential proliferative pathway in colorectal cancer stem cells - in a way alternative to EGF, which bypasses cetuximab inhibition. As the effect of NRG1 on colorectal cancer stem-like cells has been only preliminarily characterized (33), we investigated its ability to sustain xenosphere propagation. Six $KRAS^{wt}$-Ctx-S xenospheres were long-term cultured either in

the standard medium or in the corresponding medium where EGF was replaced by NRG1. Beside a stronger ERK and AKT activation by NRG1, as compared with EGF (Supplementary Fig. S3D and data not shown), no significant differences were observed in the long-term proliferative potential (not shown) and, interestingly, even in the global gene expression profiles (Supplementary Fig. S4), suggesting that NRG1 could be interchangeable with EGF to support xenosphere expansion.

RNAseq analysis of xenopatients unveiled that, while most of EGF-like ligands are expressed by colorectal cancer cells, thus triggering autocrine loops, *NRG1* is seldom expressed, similarly to *HGF* (20). However, while it is known that HGF is mainly secreted by cancer-associated fibroblasts (34), the source of NRG1 is still poorly understood, although it may include bone marrow-derived mesenchymal stem cells (35) or infiltrating lymphoid cells (36). Therefore, as in the case of HGF, the immunocompromised xeno- or spheropatient can be inadequate to evaluate NRG1 contribution to cetuximab resistance.

To circumvent this limitation, two KRAS^{wt}-Ctx-S xenospheres were transduced with a lentiviral construct to induce autocrine expression of human *NRG1* (Supplementary Fig. S5A,B). In a proliferation assay, *NRG1*-expressing xenospheres grew in the absence of either EGF or bFGF, showing complete resistance to cetuximab, but gaining full sensitivity to lapatinib (Fig. 5C). The same result was obtained in cells cultured in conventional cell-line conditions (i.e. in the presence of serum and adhesion, Supplementary Fig. S5C). This effect was specific as no inhibition was observed with an unrelated MET inhibitor (JNJ-38877605, Fig. 5D). Interestingly, the specific EGFR small molecule inhibitor gefitinib induced a weaker response as compared to lapatinib (Fig. 5D), suggesting that NRG1 exerts its effect through both ERBB3/EGFR and ERBB3/ERBB2 heterodimers. As in the case of stimulation with exogenous NRG1 (Supplementary Fig. S3D), *NRG1*-expressing xenospheres displayed constitutive ERBB3 phosphorylation, and a stronger activation of both ERK and AKT/S6 kinase pathways as compared with their parental counterparts (Fig. 5E). These pathways were inhibited by lapatinib but almost unaffected by cetuximab (Fig. 5E). EGFR was activated in both *NRG1*-expressing and parental xenospheres (for the presence of EGF in basal medium), but, whereas in parental xenospheres EGFR phosphorylation was completely abrogated by cetuximab, in *NRG1*-expressing xenospheres it was inhibited only by lapatinib (Fig. 5E).

In order to simulate paracrine secretion, a murine fibroblast primary culture (derived from a xenopatient) was transduced with human *NRG1* (Supplementary Fig. S5E). Representative KRAS^{wt}-Ctx-S xenospheres were stimulated with conditioned media obtained from control and *NRG1*-expressing fibroblasts, and treated with either cetuximab or lapatinib.

Only the conditioned medium from *NRG1*-expressing fibroblasts could induce proliferation similarly to EGF, an effect inhibited by lapatinib but not by cetuximab (Supplementary Fig. S5E), as observed in the autocrine model (Fig. 5D).

Taken together, these experiments show that either autocrine or paracrine NRG1 powerfully stimulates proliferative EGFR signaling through ERBB3, and that this activity can be inhibited by the EGFR family kinase inhibitor lapatinib, but not by cetuximab.

***NRG1*-expressing KRAS^{wt} xenospheres are highly tumorigenic, and generate tumors resistant to cetuximab but sensitive to pan-HER inhibitors.**

In order to assess NRG1 ability to sustain cetuximab resistance *in vivo*, and explore ways to circumvent it, *NRG1*-expressing KRAS^{wt}-Ctx-S xenospheres (CRC0078 and CRC0059) and their parental counterparts were injected into NOD/SCID mice (Fig. 6A). These xenospheres were previously shown to form spheropatients highly sensitive to cetuximab treatment (Supplementary Fig. S6A) (5). One month after injection, *NRG1*-expressing xenospheres formed tumors that reached volumes suitable for starting treatments (~500 mm^3 for CRC0078 and ~200 mm^3 for CRC0059), while no parental xenosphere had formed detectable tumors (Fig. 6B). These appeared later, and reached volumes comparable to those expressing *NRG1* only after ~3 months (not shown), indicating that NRG1 strongly increases the xenosphere tumorigenic potential. RNA in-situ hybridization confirmed that NRG1 was highly expressed only in tumors derived from *NRG1*-expressing xenospheres (Fig. 6C). Spheropatients were then treated with cetuximab and/or lapatinib. CRC0078-NRG1 and CRC0059-NRG1 spheropatients were completely resistant to cetuxumab, as tumors grew with the same rate as controls (Fig. 6D). In contrast, the same tumors were arrested by lapatinib. No additive/synergistic effect was observed by lapatinib and cetuximab combination (Fig. 6D). Similar results (growth arrest) were observed by treating CRC0078-NRG1 xenopatients with two other pan-HER inhibitors, afatinib or neratinib (Fig, 6E), which cause irreversible inhibition of the catalytic site, and were shown to be more potent than lapatinib in ERBB2-amplified/mutated xenopatients (9,37). All three inhibitors effectively and comparably downregulated ERK and AKT signaling in tumors (Fig. 6F, Supplementary Fig. S6B). These results indicate that NRG1 can powerfully stimulate tumor growth *in vivo*, which can be arrested only by pan-HER inhibitors.

Discussion

mCRC xenopatients were fruitfully exploited by us and others as a translational platform to identify mechanisms of both primary and secondary resistance to cetuximab, and assess new targeting agents to bypass them (38). The identification of *ERBB2* amplification as a mechanism of primary cetuximab resistance (8) has been recently translated into a successful clinical trial (13).

In vitro preclinical models are required as well to investigate both genetic and non-genetic mechanisms of response and resistance to conventional and targeted therapies. In colorectal cancer, different cell cultures approaches have been developed, including (i) conventional cell lines (39,40), organoids (41-43) and spheroids (19,44-46), each displaying inherent and complementary advantages and limitations.

From mCRC xenopatients, we previously derived a small cohort of "xenospheres", showing that they retained cancer stem-like properties, and generated tumor xenografts ("spheropatients") that reproduced both the histotype and the pharmacological response to cetuximab of the corresponding xenopatients (5). Here we present an expanded cohort of 58 xenospheres, encompassing the main genetic lesions predictive of cetuximab resistance. By comparing gene expression profiles and WES analysis of a group of matched xenospheres and xenopatients, we observed a remarkable correspondence between the two models. WES analysis, in particular, showed that not only the type of genetic lesions, but also their respective allelic frequency, are passed on from xenopatients to xenospheres, indicating that xenospheres do not undergo a significant genetic drift from the original tumor. Moreover, they are also genetically stable over long-term propagation, as attested by longitudinal WES analysis of secondary xenospheres and a conventional cell line derived after extensive *in vitro* and *in vivo* passages of a prototypic case. Concerning their prerogatives as a reliable *in vitro* model, we can conclude that xenospheres display a faithful genetic correspondence with the original tumors. This genetic fidelity is shared with tumor organoids, whose derivation has been reported to be more efficient than xenospheres (90% vs. 45-50%) and whose growth, unlike that of xenospheres, tend to reproduce also cell pseudo-differentiation as in whole tumor tissues (41). However, with respect to organoids, xenospheres and, in general, cancer stem-like cells propagated in culture as spheroids, are endowed with the advantage to be more amenable to genetic manipulation and quantitative assessment of therapeutic outcomes at cancer stem cell level, either *in vitro* or after *in vivo* transplantation and tumor regeneration (5).

As previously shown by us in a limited number of cases (5), and recently observed also in tumor organoids (42), $KRAS^{mut}$ xenospheres display EGF-independent proliferative ability and, not surprisingly, are highly resistant to cetuximab *in vitro*. Here we show for the first time that also $KRAS^{wt}$ xenospheres derived from cetuximab-resistant xenopatients are mainly EGF-independent, and enriched with cases harboring genetic alterations such as *EGFR* extracellular domain mutations, *ERBB2* mutation or amplification, *BRAF* mutations, *PTEN* deletion and *IGF2* overexpression, each of which can provide a mechanistic explanation for cell-autonomous proliferation, and a therapeutic target (8-11).

Conversely, we found that $KRAS^{wt}$ xenospheres derived from cetuximab-sensitive xenopatients ($KRAS^{wt}$-Ctx-S) are devoid of genetic alterations able to hijack the proliferative pathway, and display strong EGF-dependent proliferative ability and *in vitro* cetuximab sensitivity. While representing patients that likely would benefit from anti-EGFR therapy, $KRAS^{wt}$-Ctx-S xenospheres can also be susceptible to autocrine and paracrine signals that can counteract EGFR inhibition, as we previously showed for the HGF-MET axis (5). By screening the ability of a growth factors panel to induce primary resistance to cetuximab *in vitro*, we identified different responses that can explain pre-clinical and clinical observations. In particular, among the EGF family of ligands, EREG and AREG are completely unable to outcompete the antibody. Accordingly, their expression does not confer resistance, but, rather, is associated with cetuximab response both in patients (28,29) and in xenopatients (10). Interestingly, unlike EGF, these ligands, although capable of inducing proliferation, cannot trigger EGFR internalization and degradation, suggesting that ligand-induced disappearance of EGFR from the cell surface is relevant to protect cells from cetuximab inhibition. Similarly, TGFα and HBEGF induce only partial EGFR internalization and cetuximab resistance; this correlates with their enriched expression in $KRAS^{wt}$ xenopatients displaying either complete or partial resistance (disease stabilization) to cetuximab (10).

In our study, NRG1 emerged as a pivotal factor of primary resistance to EGFR inhibition. NRG1 is a ligand of the EGF family whose role in tumors has been poorly characterized. NRG1 binds the kinase-deficient ERBB3 receptor, and induces its heterodimerization with the other family members (EGFR, ERBB2 and ERBB4), which are required for ERBB3 transphosphorylation and the ensuing signaling activity (16). The mechanism of ERBB3 activation is complex and depends also on other EGF family ligands, specifically binding EGFR, as well as on dimerization with unrelated receptors such as the HGF receptor/MET (47). By this multiple interactions, ERBB3 is involved in primary and secondary resistance to EGFR or ERBB2 inhibition in several tumor types, including lung

(47), head and neck (48), and *ERBB2*-amplified colorectal cancers (37). Concerning the specific role of NRG1, it was reported that this factor can induce *in vitro* resistance to various kinase inhibitors (26,33). In CRC, high levels of circulating NRG1 correlate with weak response to cetuximab (14). However, the activity of NRG1 has been so far poorly investigated at the mechanistic level in *in vitro* models. The ability of NRG1 to induce cetuximab resistance has been recently reported in a single conventional CRC cell line (49), which harbored a high-copy *EGFR* amplification, a genetic alteration uncommon in CRC. Our study shows for the first time the protective ability of NRG1 in a large panel of mCRC stem-like cells that faithfully mirror the genetic make-up of the original tumors, thus achieving robust translational reliability. Moreover, we provide also the first evidence that NRG1 sustains long-term *in vitro* propagation of mCRC stem-like cells.

As NRG1 is produced by still elusive cells of the tumor microenvironment (20), to investigate its ability to sustain cetuximab resistance *in vivo* we induced *NRG1* expression in $KRAS^{wt}$-Ctx-S xenospheres, as we previously did for HGF (5). *NRG1*-expressing xenospheres displayed EGF-independent proliferative ability and full resistance to cetuximab. However, they were highly sensitive to lapatinib, a pan-HER inhibitor active in cancer cell lines harboring an NRG1-autocrine loop (50). Here we show for the first time that NRG1 dramatically increases the tumorigenic potential of xenospheres injected into NOD/SCID mice. In accordance with *in vitro* data, *NRG1*-expressing spheropatients displayed complete resistance to cetuximab treatment, but high sensitivity to different pan-HER inhibitors, including lapatinib, afatinib and neratinib.

It has been previously shown that rare genetic lesions in members of the EGFR family (*EGFR* and *ERBB2* mutations, *ERBB2* amplification) promote resistance to anti-EGFR therapy in $KRAS^{wt}$ xenopatients (8,9,11) and patients (13), which can be bypassed by different strategies that ultimately target multiple ERBBs. Here, by using a large cohort of colorectal cancer stem-like cultures, we show that the same strategy might also be effective in counteracting non-genetic mechanisms of primary resistance driven by ligands of the EGFR family, mainly NRG1. These results provide a proof-of-concept for the clinical investigation of NRG1 as a predictive biomarker of primary resistance to selective EGFR targeting, suggesting the requirement for broad inhibition of the entire EGFR family. This should apply primarily to RAS^{wt} patients, and, possibly, to all patients lacking other biomarkers of resistance to EGFR inhibition, such as *K/NRAS* or *BRAF* mutations, *MET* amplification or *IGF2* overexpression. As in the patient population NRG1 expression is likely a continuous variable, its clinical development as a predictive biomarker presents with the challenge to

define a reliable threshold that discriminates positive from negative cases. As the cellular origin of NRG1 remains elusive, and likely involves tumor-associated cells, evaluation of *in-situ* expression, although feasible either with immunohistochemistry or the more sensitive RNA *in situ* hybridization, can be significantly jeopardized by sample-bias. Integration of complementary approaches including measurements in circulating blood (14) should be recommended.

Acknowledgments

We thank Raffaella Albano for technical help, Eugenia Zanella and Francesco Galimi for genomic data of xenopatients, Roberta Porporato for RNA-ISH analysis, Antonella Cignetto, Daniela Gramaglia and Francesca Natale for assistance. P.L. was recipient of a “Fondazione Umberto Veronesi” post-doctoral fellowship.

References

1. Cremolini C, Schirripa M, Antoniotti C, Moretto R, Salvatore L, Masi G, *et al.* First-line chemotherapy for mCRC—a review and evidence-based algorithm. Nat Rev Clin Oncol **2015**;12:607-19.
2. Sepulveda AR, Hamilton SR, Allegra CJ, Grody W, Cushman-Vokoun AM, Funkhouser WK, *et al.* Molecular Biomarkers for the Evaluation of Colorectal Cancer: Guideline From the American Society for Clinical Pathology, College of American Pathologists, Association for Molecular Pathology, and the American Society of Clinical Oncology. J Clin Oncol **2017**;35:1453-86.
3. Dienstmann R, Vermeulen L, Guinney J, Kopetz S, Tejpar S, Tabernero J. Consensus molecular subtypes and the evolution of precision medicine in colorectal cancer. Nat Rev Cancer **2017**;17:79-92.
4. Schneider MR, Yarden Y. The EGFR-HER2 module: a stem cell approach to understanding a prime target and driver of solid tumors. Oncogene **2016**;35:2949-60.
5. Luraghi P, Reato G, Cipriano E, Sassi F, Orzan F, Bigatto V, *et al.* MET Signaling in Colon Cancer Stem-like Cells Blunts the Therapeutic Response to EGFR Inhibitors. Cancer Res **2014**;74:1857-69.
6. Misale S, Di Nicolantonio F, Sartore-Bianchi A, Siena S, Bardelli A. Resistance to anti-EGFR therapy in colorectal cancer: from heterogeneity to convergent evolution. Cancer Discov **2014**;4:1269-80.
7. Bardelli A, Corso S, Bertotti A, Hobor S, Valtorta E, Siravegna G, *et al.* Amplification of the MET receptor drives resistance to anti-EGFR therapies in colorectal cancer. Cancer Discov **2013**;3:658-73.
8. Bertotti A, Migliardi G, Galimi F, Sassi F, Torti D, Isella C, *et al.* A molecularly annotated platform of patient-derived xenografts ("xenopatients") identifies HER2 as an effective therapeutic target in cetuximab-resistant colorectal cancer. Cancer Discov **2011**;1:508-23.
9. Kavuri SM, Jain N, Galimi F, Cottino F, Leto SM, Migliardi G, *et al.* HER2 activating mutations are targets for colorectal cancer treatment. Cancer Discov **2015**;5:832-41.
10. Zanella ER, Galimi F, Sassi F, Migliardi G, Cottino F, Leto SM, *et al.* IGF2 is an actionable target that identifies a distinct subpopulation of colorectal cancer patients with marginal response to anti-EGFR therapies. Sci Transl Med **2015**;7:272ra12.

11. Bertotti A, Papp E, Jones S, Adleff V, Anagnostou V, Lupo B, *et al.* The genomic landscape of response to EGFR blockade in colorectal cancer. Nature **2015**;526:263-7.
12. Arena S, Siravegna G, Mussolin B, Kearns JD, Wolf BB, Misale S, *et al.* MM-151 overcomes acquired resistance to cetuximab and panitumumab in colorectal cancers harboring EGFR extracellular domain mutations. Sci Transl Med **2016**;8:324ra14.
13. Sartore-Bianchi A, Trusolino L, Martino C, Bencardino K, Lonardi S, Bergamo F, *et al.* Dual-targeted therapy with trastuzumab and lapatinib in treatment-refractory, KRAS codon 12/13 wild-type, HER2-positive metastatic colorectal cancer (HERACLES): a proof-of-concept, multicentre, open-label, phase 2 trial. Lancet Oncol **2016**;17:738-46.
14. Yonesaka K, Zejnullahu K, Okamoto I, Satoh T, Cappuzzo F, Souglakos J, *et al.* Activation of ERBB2 signaling causes resistance to the EGFR-directed therapeutic antibody cetuximab. SciTranslMed **2011**;3:99ra86.
15. Harris RC, Chung E, Coffey RJ. EGF receptor ligands. Exp Cell Res **2003**;284:2-13.
16. Yarden Y, Pines G. The ERBB network: at last, cancer therapy meets systems biology. Nat Rev Cancer **2012**;12:553-63.
17. Graham J, Muhsin M, Kirkpatrick P. Cetuximab. Nat Rev Drug Discov **2004**;3:549-50.
18. Ronan T, Macdonald-Obermann JL, Huelsmann L, Bessman NJ, Naegle KM, Pike LJ. Different Epidermal Growth Factor Receptor (EGFR) Agonists Produce Unique Signatures for the Recruitment of Downstream Signaling Proteins. J Biol Chem **2016**;291:5528-40.
19. Boccaccio C, Luraghi P, Comoglio PM. MET-mediated resistance to EGFR inhibitors: an old liaison rooted in colorectal cancer stem cells. Cancer Res **2014**;74:3647-51.
20. Isella C, Terrasi A, Bellomo SE, Petti C, Galatola G, Muratore A, *et al.* Stromal contribution to the colorectal cancer transcriptome. Nat Genet **2015**;47:312-9.
21. Isella C, Brundu F, Bellomo SE, Galimi F, Zanella E, Porporato R, *et al.* Selective analysis of cancer-cell intrinsic transcriptional traits defines novel clinically relevant subtypes of colorectal cancer. Nat Commun **2017**;8:15107.
22. Network TCGA. Comprehensive molecular characterization of human colon and rectal cancer. Nature **2012**;487:330-7.
23. Williams MJ, Werner B, Barnes CP, Graham TA, Sottoriva A. Identification of neutral tumor evolution across cancer types. Nat Genet **2016**;48:238-44.
24. Sottoriva A, Kang H, Ma Z, Graham TA, Salomon MP, Zhao J, *et al.* A Big Bang model of human colorectal tumor growth. Nat Genet **2015**;47:209-16.

25. Prahallad A, Sun C, Huang S, Di Nicolantonio F, Salazar R, Zecchin D, *et al.* Unresponsiveness of colon cancer to BRAF(V600E) inhibition through feedback activation of EGFR. Nature **2012**;483:100-3.
26. Harbinski F, Craig VJ, Sanghavi S, Jeffery D, Liu L, Sheppard KA, *et al.* Rescue screens with secreted proteins reveal compensatory potential of receptor tyrosine kinases in driving cancer growth. Cancer Discov **2012**;2:948-59.
27. Wilson TR, Fridlyand J, Yan Y, Penuel E, Burton L, Chan E, *et al.* Widespread potential for growth-factor-driven resistance to anticancer kinase inhibitors. Nature **2012**;487:505-9.
28. Khambata-Ford S, Garrett CR, Meropol NJ, Basik M, Harbison CT, Wu S, *et al.* Expression of epiregulin and amphiregulin and K-ras mutation status predict disease control in metastatic colorectal cancer patients treated with cetuximab. J Clin Oncol **2007**;25:3230-7.
29. Jacobs B, De Roock W, Piessevaux H, Van Oirbeek R, Biesmans B, De Schutter J, *et al.* Amphiregulin and epiregulin mRNA expression in primary tumors predicts outcome in metastatic colorectal cancer treated with cetuximab. J Clin Oncol **2009**;27:5068-74.
30. Mutsaers AJ, Francia G, Man S, Lee CR, Ebos JM, Wu Y, *et al.* Dose-dependent increases in circulating TGF-alpha and other EGFR ligands act as pharmacodynamic markers for optimal biological dosing of cetuximab and are tumor independent. Clin Cancer Res **2009**;15:2397-405.
31. Wang Q, Chen X, Wang Z. Dimerization drives EGFR endocytosis through two sets of compatible endocytic codes. J Cell Sci **2015**;128:935-50.
32. Tomas A, Futter CE, Eden ER. EGF receptor trafficking: consequences for signaling and cancer. Trends Cell Biol **2014**;24:26-34.
33. Prasetyanti PR, Capone E, Barcaroli D, D'Agostino D, Volpe S, Benfante A, *et al.* ErbB-3 activation by NRG-1β sustains growth and promotes vemurafenib resistance in BRAF-V600E colon cancer stem cells (CSCs). Oncotarget **2015**;6:16902-11.
34. Cirri P, Chiarugi P. Cancer-associated-fibroblasts and tumour cells: a diabolic liaison driving cancer progression. Cancer Metastasis Rev **2012**;31:195-208.
35. De Boeck A, Pauwels P, Hensen K, Rummens JL, Westbroek W, Hendrix A, *et al.* Bone marrow-derived mesenchymal stem cells promote colorectal cancer progression through paracrine neuregulin 1/HER3 signalling. Gut **2013**;62:550-60.

36. Uhlén M, Fagerberg L, Hallström BM, Lindskog C, Oksvold P, Mardinoglu A, *et al.* Proteomics. Tissue-based map of the human proteome. Science **2015**;347:1260419.

37. Leto SM, Sassi F, Catalano I, Torri V, Migliardi G, Zanella ER, *et al.* Sustained Inhibition of HER3 and EGFR Is Necessary to Induce Regression of HER2-Amplified Gastrointestinal Carcinomas. Clin Cancer Res **2015**;21:5519-31.

38. Byrne AT, Alférez DG, Amant F, Annibali D, Arribas J, Biankin AV, *et al.* Interrogating open issues in cancer precision medicine with patient-derived xenografts. Nat Rev Cancer **2017**;17:254-68.

39. Medico E, Russo M, Picco G, Cancelliere C, Valtorta E, Corti G, *et al.* The molecular landscape of colorectal cancer cell lines unveils clinically actionable kinase targets. Nat Commun **2015**;6:7002.

40. Ashraf SQ, Nicholls AM, Wilding JL, Ntouroupi TG, Mortensen NJ, Bodmer WF. Direct and immune mediated antibody targeting of ERBB receptors in a colorectal cancer cell-line panel. Proc Natl Acad Sci U S A **2012**;109:21046-51.

41. van de Wetering M, Francies HE, Francis JM, Bounova G, Iorio F, Pronk A, *et al.* Prospective derivation of a living organoid biobank of colorectal cancer patients. Cell **2015**;161:933-45.

42. Fujii M, Shimokawa M, Date S, Takano A, Matano M, Nanki K, *et al.* A Colorectal Tumor Organoid Library Demonstrates Progressive Loss of Niche Factor Requirements during Tumorigenesis. Cell Stem Cell **2016**;18:827-38.

43. Schütte M, Risch T, Abdavi-Azar N, Boehnke K, Schumacher D, Keil M, *et al.* Molecular dissection of colorectal cancer in pre-clinical models identifies biomarkers predicting sensitivity to EGFR inhibitors. Nat Commun **2017**;8:14262.

44. De Angelis ML, Zeuner A, Policicchio E, Russo G, Bruselles A, Signore M, *et al.* Cancer Stem Cell-Based Models of Colorectal Cancer Reveal Molecular Determinants of Therapy Resistance. Stem Cells Transl Med **2016**;5:511-23.

45. Todaro M, Alea MP, Di Stefano AB, Cammareri P, Vermeulen L, Iovino F, *et al.* Colon cancer stem cells dictate tumor growth and resist cell death by production of interleukin-4. Cell Stem Cell **2007**;1:389-402.

46. Vermeulen L, Todaro M, de Sousa MF, Sprick MR, Kemper K, Perez AM, *et al.* Single-cell cloning of colon cancer stem cells reveals a multi-lineage differentiation capacity. Proc NatlAcadSciUSA **2008**;105:13427-32.

47. Engelman JA, Zejnullahu K, Mitsudomi T, Song Y, Hyland C, Park JO, *et al.* MET amplification leads to gefitinib resistance in lung cancer by activating ERBB3 signaling. Science **2007**;316:1039-43.

48. Wang D, Qian G, Zhang H, Magliocca KR, Nannapaneni S, Amin AR, *et al.* HER3 Targeting Sensitizes HNSCC to Cetuximab by Reducing HER3 Activity and HER2/HER3 Dimerization: Evidence from Cell Line and Patient-Derived Xenograft Models. Clin Cancer Res **2017**;23:677-86.

49. Kawakami H, Okamoto I, Yonesaka K, Okamoto K, Shibata K, Shinkai Y, *et al.* The anti-HER3 antibody patritumab abrogates cetuximab resistance mediated by heregulin in colorectal cancer cells. Oncotarget **2014**;5:11847-56.

50. Wilson TR, Lee DY, Berry L, Shames DS, Settleman J. Neuregulin-1-mediated autocrine signaling underlies sensitivity to HER2 kinase inhibitors in a subset of human cancers. Cancer Cell **2011**;20:158-72.

Figure Legends

Figure 1. Derivation of a molecularly annotated xenospheres biobank.

A, Xenospheres were derived from tumor samples of patients with metastatic colorectal cancers previously implanted into immunocompromised mice and expanded as patient-derived xenografts (xenopatients). Xenosphere transplantation into immunocompromised mice (spheropatient) regenerates phenocopies of original tumors. **B**, Pie chart representing the relative distribution of genetic lesions in the total panel of 58 xenospheres (left) and in the 32 quadruple WT xenospheres (right). The number of cases harboring each genetic alteration is indicated. WT: wild-type; mut: mutation; high: overexpression; ampl: amplification; ecd: mutation in the extracellular domain; del: deletion. **C**, Heatmap representing the Pearson correlation of gene expression profiles of 28 matched xenospheres and xenopatients (GEO accession number GSE101792).

Figure 2. Whole exome sequencing analysis (WES) unveils faithful genetic correspondence between xenospheres and original xenopatients.

A, Schematic representation of WES analysis comparison between xenospheres and xenopatients. **B**, **C,** Histograms representing the total number of copy number variations (CNV, **B**) and somatic mutations (**C**) observed in xenospheres (blue columns) and xenopatients (red columns), and those shared between them (green columns). **D**, Histogram representing the average allelic frequencies of somatic mutations either private or shared in xenospheres (blue/light blue columns) and xenopatients (red/orange columns). **E**, Graph representing the correlated allelic frequency of somatic mutations shared between xenospheres and xenopatients. Each dot represents a gene mutation. Pearson correlation between allelic frequencies in xenospheres vs. xenopatients is indicated.

Figure 3. Longitudinal WES analysis of different CRC0078 xenospheres unveils *in vitro* genetic stability.

A, Schematic representation of the derivation of secondary CRC0078^{2nd} xenospheres, and CRC0078^{Ad} xenosphere-derived adherent cultures. **B**, **C,** Histogram representing the total number of copy number variations (CNV, **B**) and somatic mutations (**C**) observed in CRC0078 xenospheres, CRC0078^{2nd} xenospheres, and CRC0078^{Ad} cultures (blue columns), as compared with the original CRC0078 xenopatient (red columns), and the number of alterations shared between each *in vitro* model and the xenopatient (green columns). **D,**

Histogram representing the average allelic frequencies of somatic mutations either private (light blue columns) or shared (blue columns) with the original xenopatient, in CRC0078 xenospheres, CRC0078^{2nd} xenospheres and CRC0078^{Ad} cultures. **E,F,** Graphs representing the correlated allelic frequency of somatic mutations shared between each different *in vitro* model and the original xenopatient (**E**), and between the three different *in vitro* models (**F**). Each dot represents a gene mutation.

Figure 4. The xenosphere response to cetuximab correlates with genetic and non-genetic biomarkers of resistance.

A, Waterflow plot of the *in vitro* cetuximab response of a panel of 46 xenospheres. Cell viability was measured in xenospheres kept for 4 days in basal medium (with 0,4 ng/ml of EGF) and treated with cetuximab (10 μg/ml) or vehicle. Columns represent relative viability of xenospheres treated with cetuximab vs. vehicle. Relative viability > 0.5 (dotted line) indicates resistance, < 0.5 indicates sensitivity. Colors indicate the mutational status, as indicated in the legend. **B**, Pie charts of the genetic classification of KRAS^{wt} xenospheres (n = 30), which are subdivided in two groups according to the annotation of the cetuximab response of the original xenopatients. Left: group derived from cetuximab-resistant (Ctx-R, n = 12) xenopatients. Right: group derived from cetuximab-sensitive xenopatients (Ctx-S, n = 18). **C,** Cell viability assay of CRC0104, CRC0480 and CRC0151 xenospheres kept for 4 days in stem-cell medium without any growth factor (NoGF) or with 0,4 ng/ml of EGF (Basal Medium), and treated as indicated (cetuximab 10 μg/ml, panitumumab 10 μg/ml, gefitinib 0,5 μM, Lapatinib 0,5 μM, PLX4720 2 μM). Columns represent the relative viability vs. vehicle (No GF) ± s.e.m (*n* = 3). **D**, **E,** Cell viability assay of KRAS^{wt} Ctx-R (n=12, C) or KRAS^{wt} Ctx-S (n=18, D) xenospheres kept for 4 days in basal medium alone (with 0,4 ng/ml of EGF), or supplemented with 20 ng/ml of the indicated growth factors, and treated with cetuximab (10 μg/ml) or vehicle. Dots represent the ratio of raw viability data between cetuximab-treated and vehicle-treated xenospheres. Each dot represents one single xenosphere. Red line: mean value for the group. Statistical analysis of the assay was performed with one-way ANOVA (p<0,0001). Bonferroni Multiple Comparison Test was applied to compare each growth factor with basal medium (**p<0,01; ***p<0,001).

Figure 5. EGF family ligands differently modulate EGFR activity and cetuximab response

A, Western Blot analysis of total protein extracts from CRC0078 xenospheres cultured for 24 h in stem-cell medium containing either of the indicated EGF-like ligands (20 ng/ml). **B**, Flow cytometric analysis of EGFR and ERBB3 in CRC0078 xenospheres cultured as described in A. **C**, Growth curves of CRC0078-NRG1 xenospheres kept in basal stem cell medium without any growth factor and treated either with vehicle, cetuximab (10 μg/ml) or lapatinib (0,5 μM). Graphs represent the relative viability increase vs. day 0 ± s.e.m (*n* = 3). Statistical analysis of the assay was performed with one-way ANOVA (p<0,0001). Bonferroni Multiple Comparison Test was applied to compare each treatment with vehicle (***p<0,001). **D**, Cell viability of CRC0078-NRG1 xenospheres kept for 4 days in basal stem cell medium without any growth factor and treated either with vehicle, cetuximab (10 μg/ml), gefitinib (0,5 μM), lapatinib (0,5 μM) or JnJ-38877605 (0,5 μM). Columns represent relative cell viability vs. vehicle ± s.e.m (*n* = 3) Statistical analysis was performed with one-way ANOVA (p<0,0001). Bonferroni Multiple Comparison Test was applied to compare treatment with vehicle (***p<0,001). **E**, Western Blot analysis of total protein extracts from CRC0059 and CRC0078 parental and NRG1-expressing xenospheres cultured either in the absence of any growth factor (No GF), or with 0,4 ng/ml of EGF (basal medium) and treated either with vehicle, cetuximab (10 μg/ml), lapatinib (0,5 μM) or their combination (combo) in basal medium.

Figure 6. NRG1-expressing KRAS^{wt}-Ctx-S spheropatients are highly tumorigenic, and generate tumors resistant to cetuximab but sensitive to pan-HER inhibitors.

A, Schematic representation of the generation of spheropatients by KRAS^{wt}-Ctx-S and *NRG1*-expressing KRAS^{wt}-Ctx-S xenospheres. **B**, Graph representing the distribution of CRC0059 and CRC0078 parental or *NRG1* expressing spheropatient tumor volumes one month after xenosphere injection (5×10^4 cells/mouse). Red line: Mean Value. Statistical analysis was performed using one-way ANOVA (p<0,0001). **C**, Micrographs of *NRG1* RNA in Situ Hybridization (ISH) performed on histological tumor sections derived from CRC0059 and CRC0078 parental or *NRG1* expressing spheropatients. Magnification: 20X. **D**, Tumor growth curves of CRC0059-NRG1 and CRC0078-NRG1 spheropatients treated as indicated. Graphs represent tumor volume increase vs. day 0 ± s.e.m. (*n* = 6/group). Statistical analysis was performed using one-way ANOVA (p=0,004 for CRC0078; p<0,0001 for CRC0059). Bonferroni Multiple Comparison Test was applied to compare treatments with vehicle

(**p<0,01, ***p<0,001) **E**, Growth curves of CRC0078-NRG1 spheropatients treated as indicated. Graphs represent tumor volume increase vs. day 0 ± s.e.m. (*n* = 4/group). **F**, Immunohistochemical analysis with anti-pERK or anti-pS6 antibodies of histological tumor sections derived from CRC0078-NRG1 spheropatients treated as indicated for 3 weeks. Magnification: 20X.

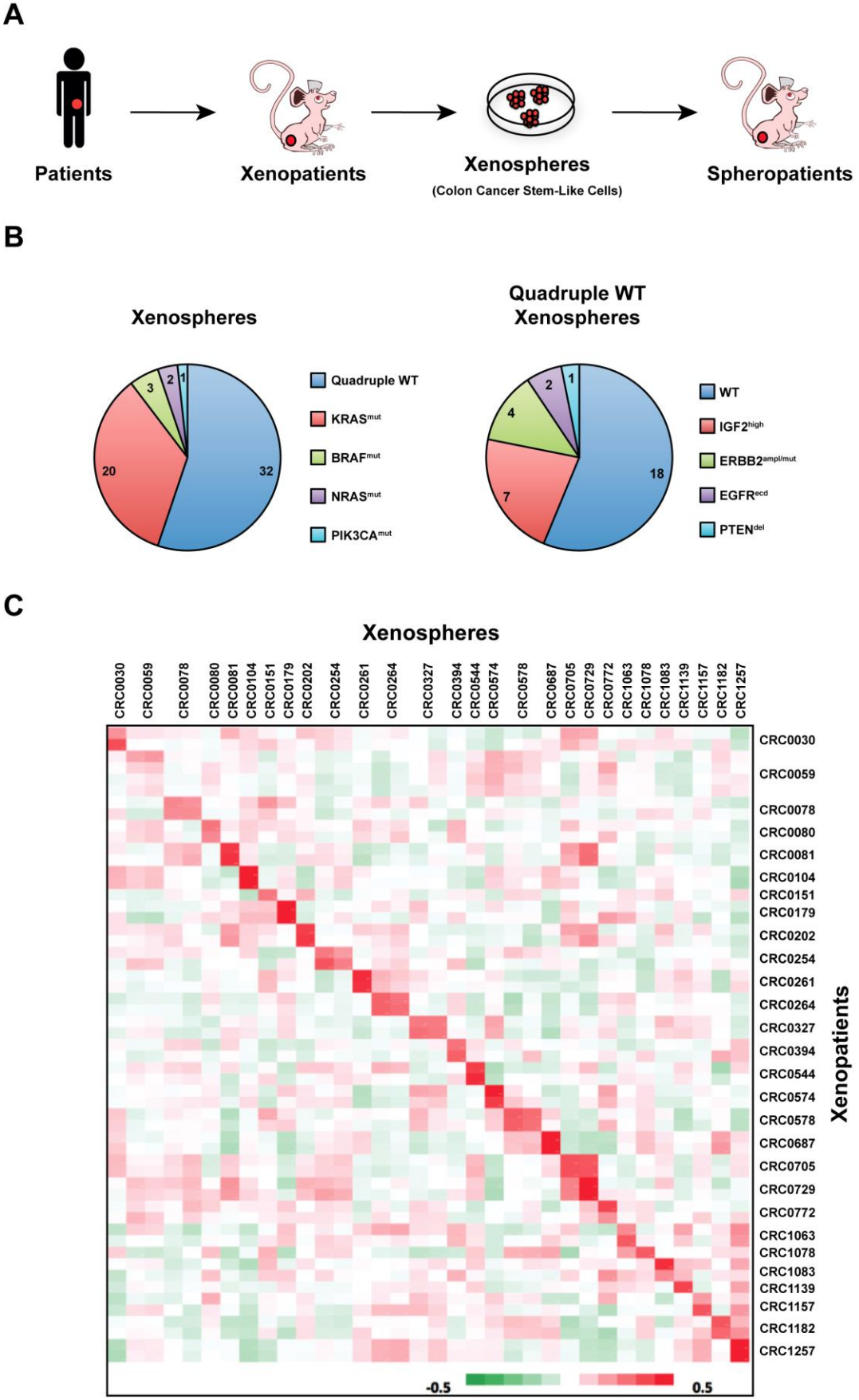

Luraghi et al., Figure 1

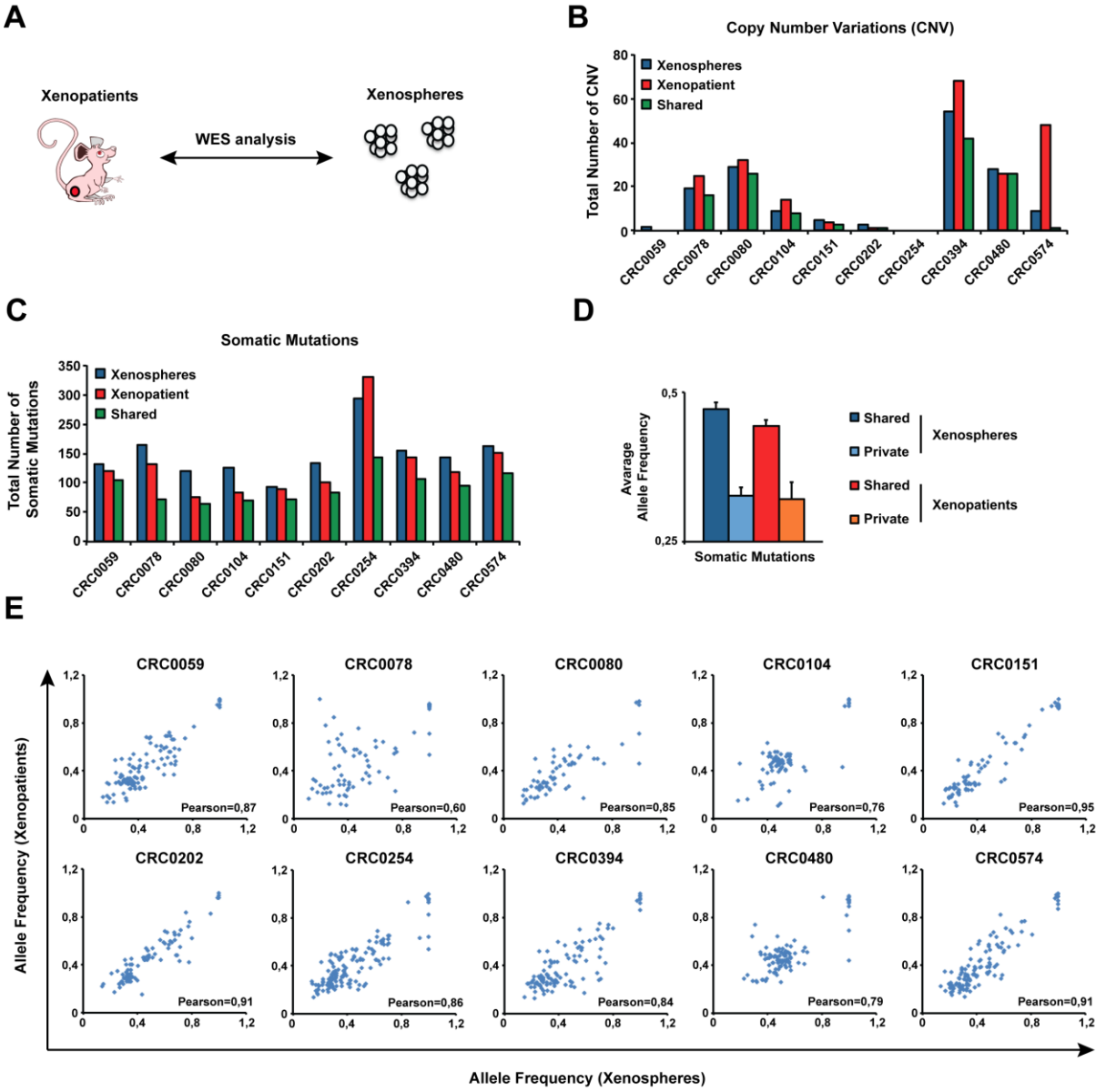

Luraghi et al., Figure 2

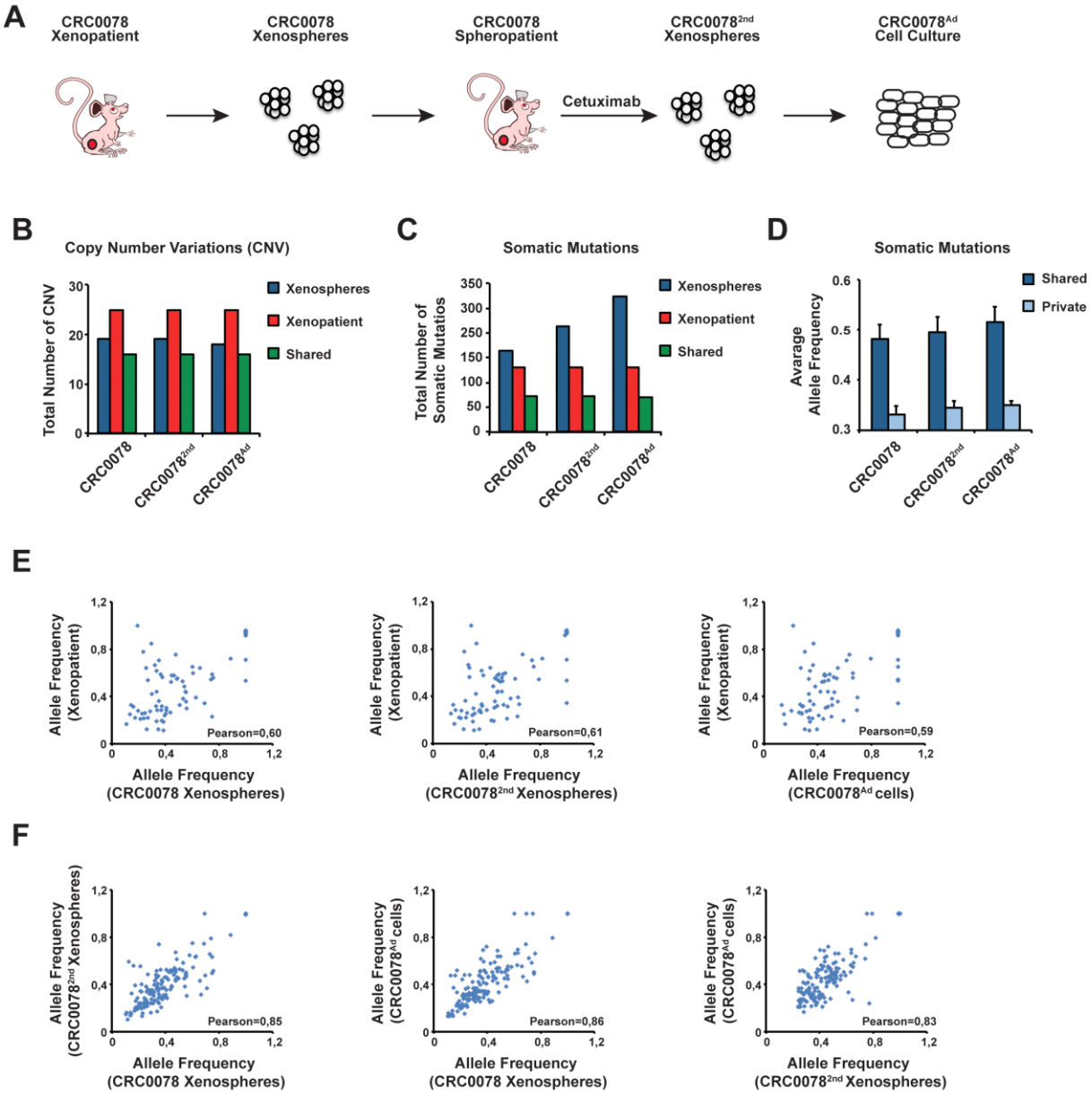

Luraghi et al., Figure 3

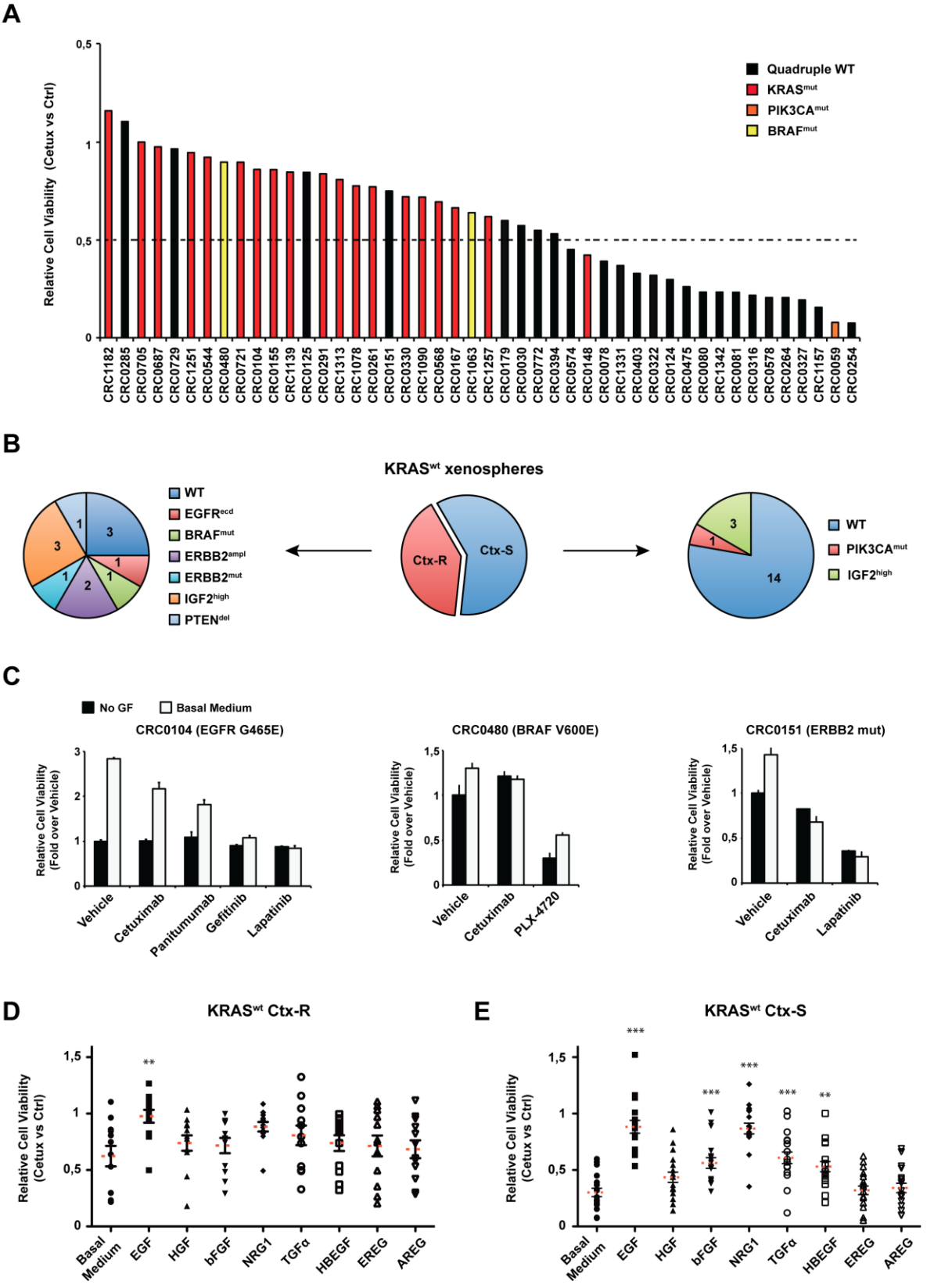

Luraghi et al., Figure 4

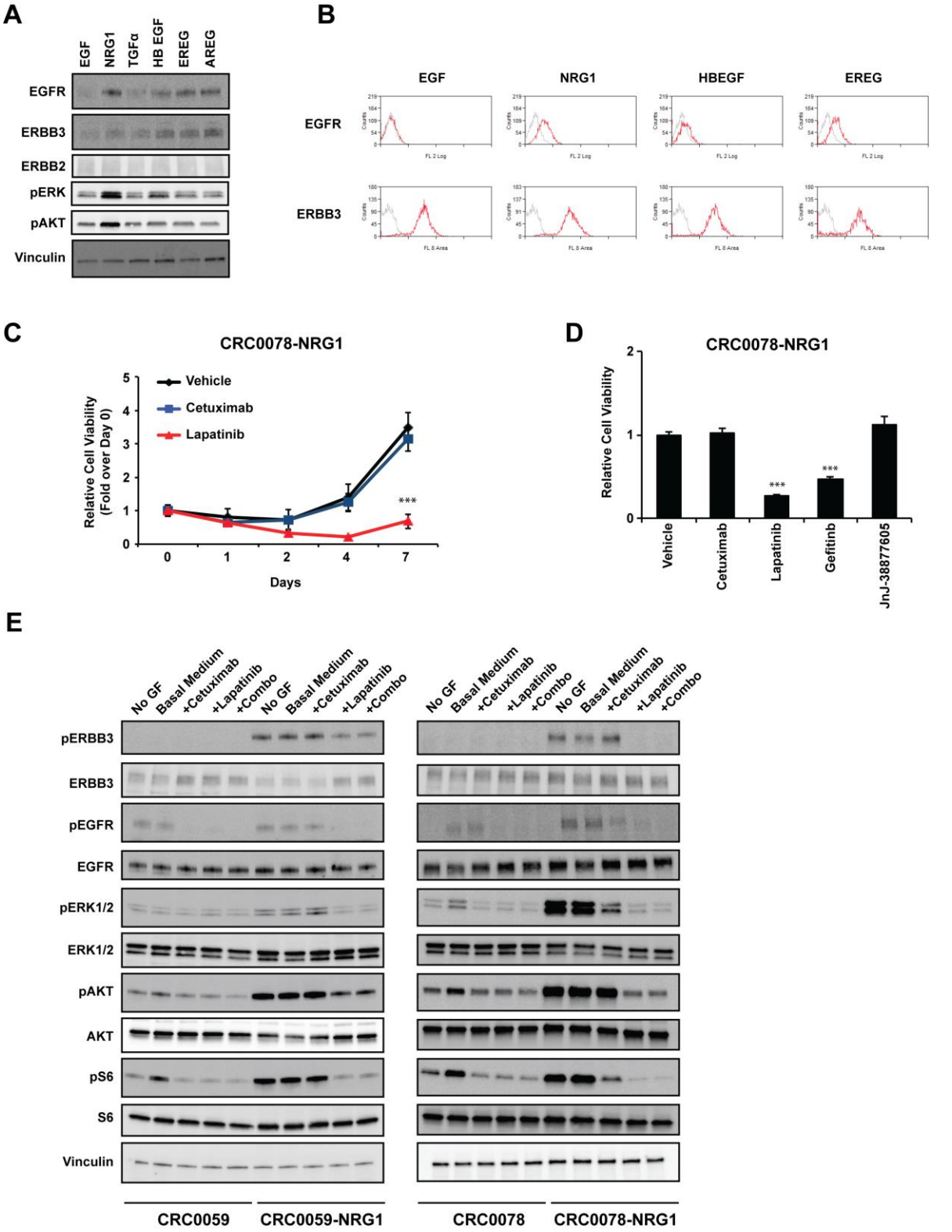

Luraghi et al., Figure 5

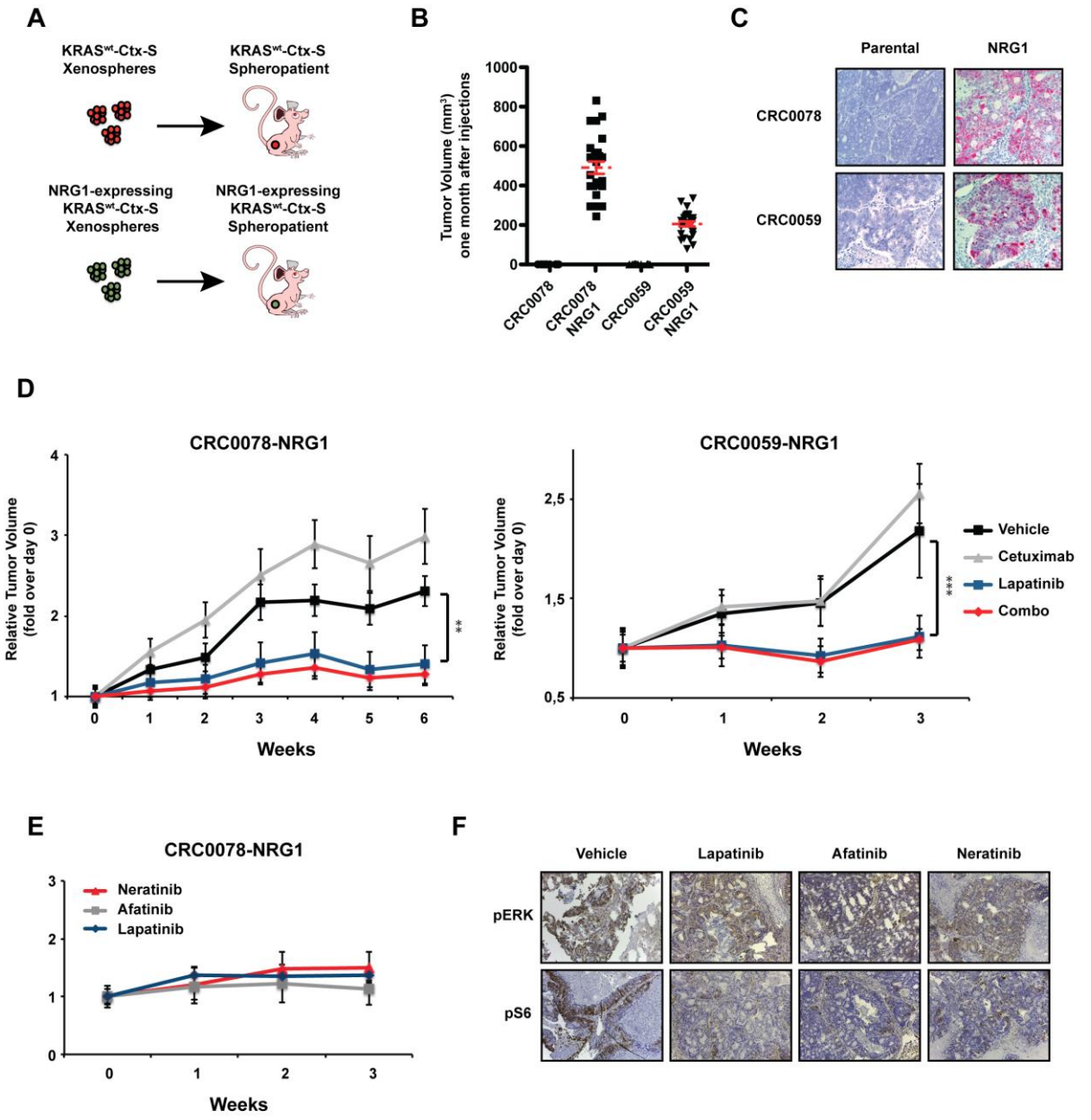

Luraghi et al., Figure 6

Supplementary Experimental Procedures

Tumor dissociation and xenosphere generation

Xenopatients were obtained as described (8) and their tumors were mechanically dissociated, digested with Type-I Collagenase (1 mg/ml, Life Technologies-Invitrogen), filtered through a 70 µm cell strainer (BD Falcon), and cleared with histopaque-1077 (Sigma), according to manufacturer instructions. Cells were grown in ultra-low attachment plastics (Sigma-Corning) in standard stem-cell medium. This included human recombinant epidermal growth factor (EGF, 20 ng/ml; Sigma), basic fibroblast growth factor 2 (bFGF, 10 ng/ml; Peprotech), added to stem cell medium, i.e. DMEM/F-12 (Sigma) supplemented with 2 mM glutamine (Sigma), penicillin-streptomycin (1:100, EuroClone), N-2 supplements (Life Technologies-GIBCO), 0.4% BSA (Sigma), 4 µg/ml heparin (Sigma), CD Lipid Concentrate (Life Technologies-GIBCO). Cells were kept in humidified incubators at 37°C, with 5% O_2 and 5% CO_2.

Genomic DNA extraction and mutational screening

Genomic DNA was extracted with the Wizard® SV genomic DNA purification system (Promega) according to the manufacturer's instructions. The quality of nucleic acids was verified by measuring the 260/280 absorbance ratio with ND-1000 V3.7.1 Nanodrop (Thermo Scientific). Purified gDNA was analyzed for KRAS, NRAS, BRAF, PIK3CA, as previously described (8).

Microarray data generation and processing

RNA was extracted using the miRNeasy Mini Kit (Qiagen), according to the manufacturer's intructions. Synthesis of cDNA and biotinylated cRNA (from 500 ng total RNA) was performed using the IlluminaTotalPrep RNA Amplification Kit (Ambion), according to the manufacturer's instuctions. Quality assessment and quantitation of total RNA and cRNAs were performed with Agilent RNA kits on a Bioanalyzer 2100 (Agilent). Hybridization of cRNAs (750 ng) was carried out using Illumina Human 48k gene chips (Human HT-12 V4 BeadChip). Array washing was performed by Illumina High Temp Wash Buffer for 10' at 55°C, followed by staining using streptavidin-Cy3 dyes (Amersham Biosciences). Hybridized arrays were stained and scanned in a Beadstation 500 (Illumina).

Probe intensity data were extracted using the Illumina Genome Studio software (Genome Studio V2011.1) and subjected to Loess normalization using the Lumi R package. To minimize the noise due to cross-species hybridization of transcripts deriving from murine infiltrates in PDX tissues, two pure murine samples were hybridized on human arrays in a pilot experiment, and all probes that generated detectable signals in this assay were removed from further analyses. Probes were filtered

to select those that showed detectable signal (detection P value = 0) in at least one samples. For each of such genes, only the probe with the highest variance of signal was selected. Pearson's correlations were performed for any possible PDX/Xenosphere permutation. The dataset was uploaded on the GEO Database (GEO accession number GSE101792).

Generation of NRG1-expressing xenopheres

To generate stable xenospheres (M016 and M049) or murine fibroblasts expressing NRG1, cells were transduced with a lentiviral vector generated by transfecting 293-T cells with different plasmids: the packaging construct encodes the HIV-1 Gag and Pol precursors, the regulatory proteins Tat and Rev, pMDL, the VSV-G expressing construct, and the transfer construct OriGene's TrueORF clone RC220134L1V (Origene). The ORF cloned in this vector was expressed as a tagged protein with c-terminal Myc-DDK tags.

Real time RT-PCR

Total RNA was extracted using miRNAeasy mini Kit according to manufacturer's instructions (Qiagen). 1 µg of purified RNA was used as a template for cDNA synthesis with random and hexamer primers and high capacity reverse transcription kit (Applied Biosystem). To evaluate NGR1 expression Real-time PCR was performed using TaqMan® Universal Master Mix (Life Technologies) containing 200 ng of cDNA and a TaqMan® gene expression probe Hs00247620_m1 on ABI PRISM 7900HT sequence detection system. Relative quantification value for NGR1 gene expression was obtained by normalizing to ubiquitin and beta actin as endogenous controls. All samples were run in triplicate and the mean and standard deviation calculated.

Murine Fibroblast Conditioned Medium (mFIBR CM)

A murine fibroblast culture derived from a xenopatient was isolated and transduced to express human NRG1 as described above. Cells were plated in adhesive dishes in DMEM supplemented with 2 mM glutamine, penicillin-streptomycin, and 10% FBS. To obtain mFIBR CM, fibroblasts were grown up to confluence and then kept for 24h in basal stem-cell medium.

Western Blotting

Xenospheres protein expression were analyzed on whole-cell lysates, solubilized in boiling Laemmli buffer. For spheropatient protein expression, snap-frozen tissues were mechanically dissociated and solubilized with EB-extraction buffer (20 mMTris-HCl pH 7.4, 150 mM NaCl, 10% Glycerol, 1% TritonX-100, 5mM EDTA) in the presence of protease and phosphatase inhibitors.

Protein concentration was determined using a BCA Protein Assay Reagent kit (Pierce Biotechnology). Equal amounts of proteins were resolved by SDS-PAGE in reducing conditions and analyzed by immunoblotting. Antibodies were visualized with appropriate horseradish peroxidase-conjugated secondary antibodies (Amersham), and the enhanced chemioluminescence system (ECL, Amersham). Blot images were captured using the FujiFilm LAS-3000 digital imaging system.

Immunohistochemistry

Tumors explanted from mice were formalin-fixed and paraffin-embedded according to standard procedures. 4 µm tissue sections were dried in a 37°C oven overnight. Slides were de-paraffinized in xylene and rehydrated through graded alcohol to water. Endogenous peroxidase was blocked in 3% hydrogen peroxide for 30 minutes. Microwave antigen retrieval was carried out using a microwave oven (750 W for 10 minutes) in 10 mmol/L citrate buffer, pH 6.0. Slides were incubated with individual primary antibodies overnight at 4°C inside a moist chamber. After washings in TBS, anti-rabbit secondary antibody (DakoEnvision+System-horseradish peroxidase–labeled polymer, Dako) was added. Incubations were carried out for 1 hour at room temperature. Immunoreactivities were revealed by incubation in DAB chromogen (DakoCytomation Liquid DAB Substrate Chromogen System, Dako) for 10 minutes. Slides were counterstained in Mayer's hematoxylin, dehydrated in graded alcohol, cleared in xylene, and the coverslip was applied by using DPX. A negative control slide was processed with secondary antibody, omitting primary antibody incubation. Images were captured with the LEICA LAS EZ software with the use of a LEICA ICC50 HD microscope.

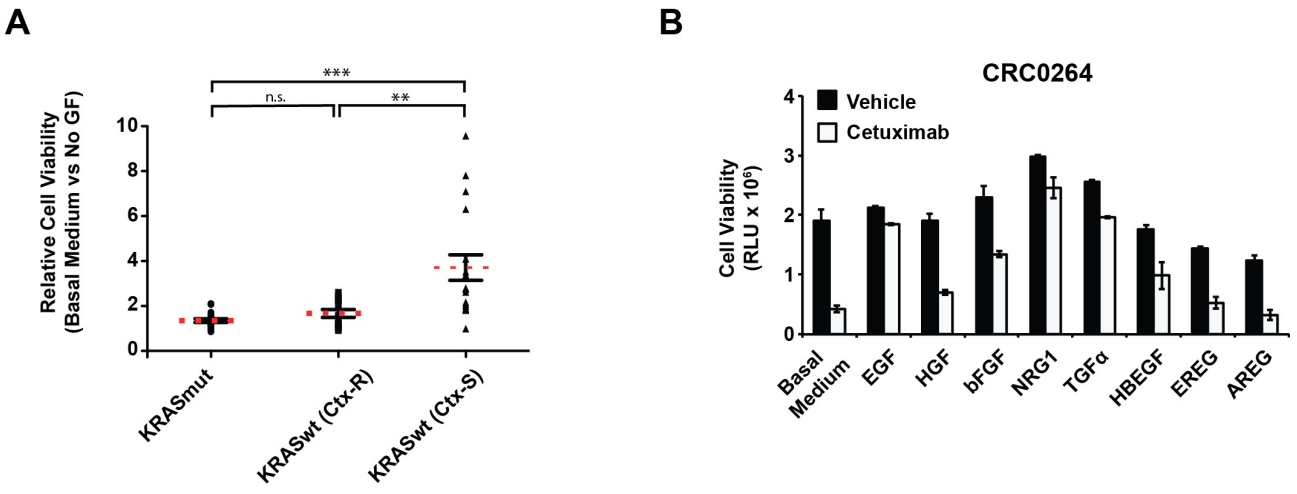

Supplementary Figure 1.

A, Cell viability assay of KRAS^{mut} (n=18), KRAS^{wt} Ctx-R (n=12) and Ctx-S (n=18) xenospheres kept for 4 days in basal stem-cell medium without any growth factor (No GF) or with 0,4 ng/ml of EGF (Basal Medium). Dots represent the ratio of raw viability data between EGF and NoGF. Red line: mean value for the group. Statistical analysis was performed with one-way ANOVA (p<0,0001). Bonferroni Multiple Comparison Test was applied to compare each group (n.s.=not significative; **p<0,01; ***p<0,001). **B**, Cell viability assay of CRC0264 xenospheres kept for 4 days in basal stem-cell medium containing 0,4 ng/ml of EGF (basal medium) or 20 ng/ml of the indicated growth factors, and treated with cetuximab (10 µg/ml) or vehicle. Columns represent raw viability data.

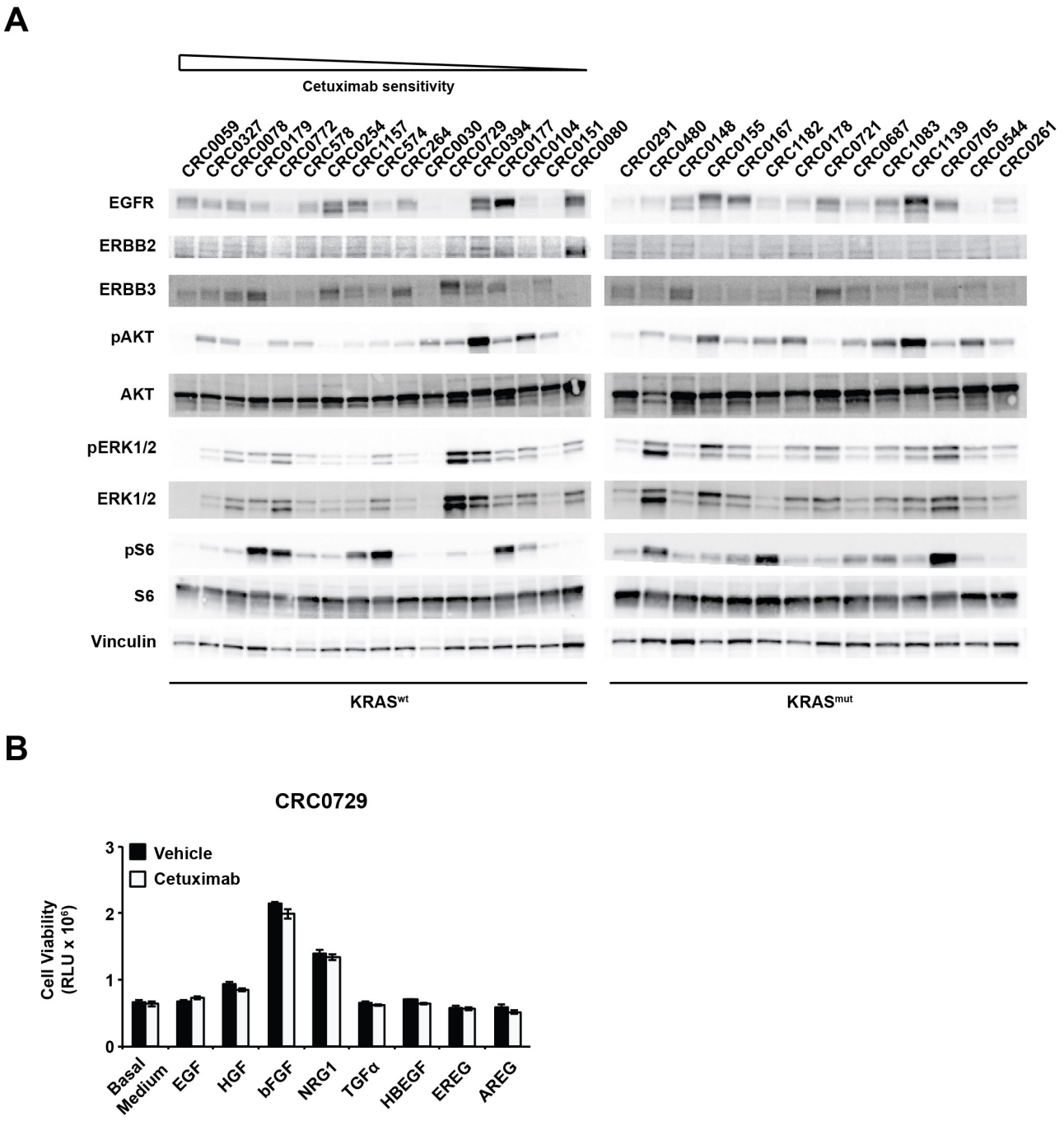

Supplementary Figure 2.

A, Western Blot analysis of total protein extracts from the indicated KRAS^{wt} and KRAS^{mut} xenospheres cultured in standard stem-cell medium (i.e. containing 20 ng/ml of EGF and 10 ng/ml bFGF). **B**, Cell viability assay of CRC0729 xenospheres kept for 4 days in basal stem-cell medium

containing 0,4 ng/ml of EGF (Basal Medium) or 20 ng/ml of the indicated growth factors, and treated with cetuximab (10 μg/ml) or vehicle. Columns represent raw RLU data.

A

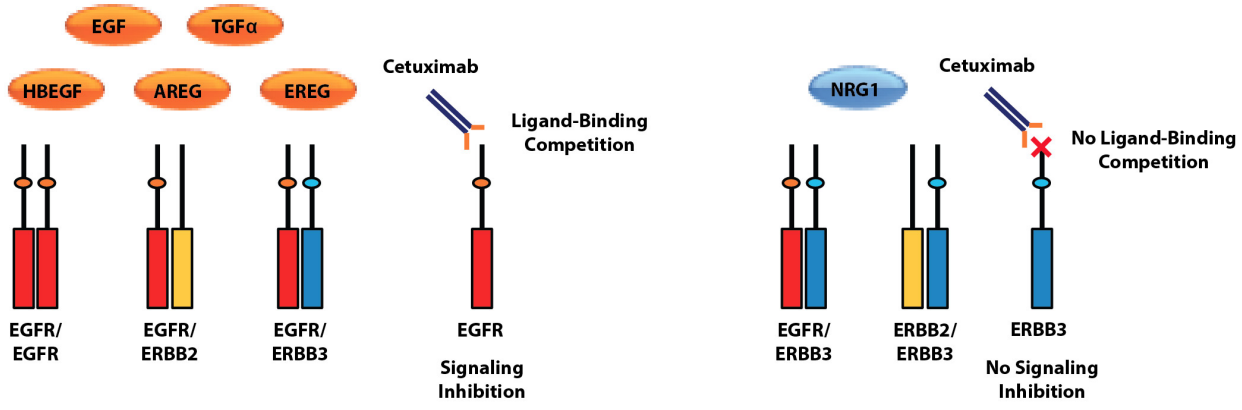
EGF
TGFα
HBEGF
AREG
EREG
Cetuximab
Ligand-Binding Competition
EGFR/ EGFR
EGFR/ ERBB2
EGFR/ ERBB3
EGFR
Signaling Inhibition
NRG1
Cetuximab
No Ligand-Binding Competition
EGFR/ ERBB3
ERBB2/ ERBB3
ERBB3
No Signaling Inhibition

B

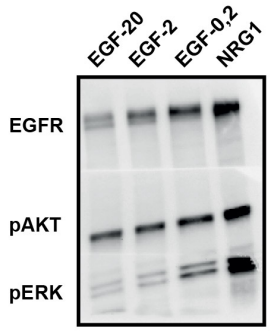
EGF-20
EGF-2
EGF-0,2
NRG1
EGFR
pAKT
pERK

C

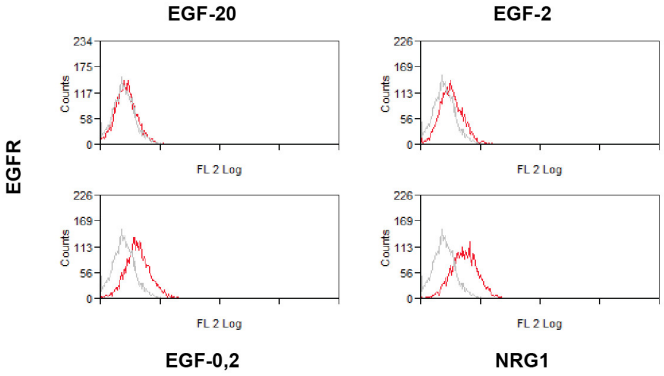
EGF-20
EGF-2
EGF-0,2
NRG1
EGFR
Counts
FL 2 Log

D

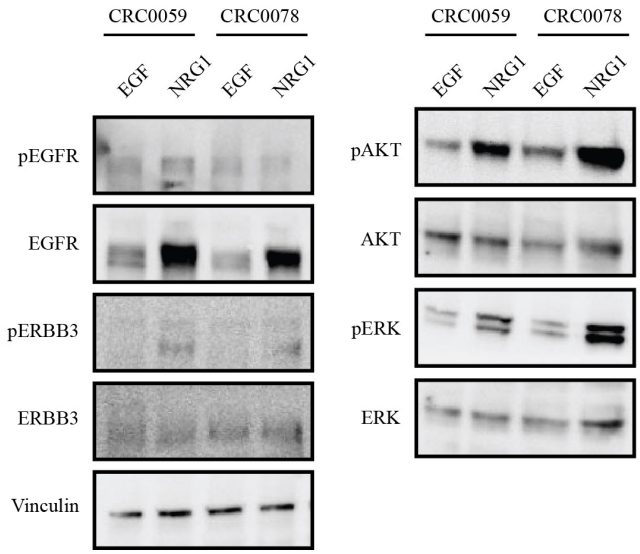
CRC0059
CRC0078
EGF
NRG1
EGF
NRG1
pEGFR
EGFR
pERBB3
ERBB3
Vinculin
CRC0059
CRC0078
EGF
NRG1
EGF
NRG1
pAKT
AKT
pERK
ERK

Supplementary Figure 3.

A, Schematic representation of binding properties of the EGF family ligands in xenospheres. In orange, EGF-like ligands that bind EGFR and induce formation of three different receptor heterodimers, all containing EGFR (red: EGFR, yellow: ERBB2, blue: ERBB3). Cetuximab is likely to inhibit dimer formation by outcompeting these ligands. In blue, NRG1 binds ERBB3 and induces two different heterodimers, which are not inhibited by cetuximab as this does not compete with NRG1 for ERBB3 binding. **B**, Western Blot analysis of total protein extracts from CRC0078 xenospheres kept for 4 days in basal stem-cell medium containing 0.2, 2 or 20 ng/ml of EGF. **C**, Flow cytometric analysis of EGFR on CRC0078 xenospheres cultured as described in B. **D**, Western Blot analysis of total protein extracts from CRC0059 and CRC0078 xenospheres long-termed cultured in stem-cell medium containing either EGF or NRG1 (20 ng/ml).

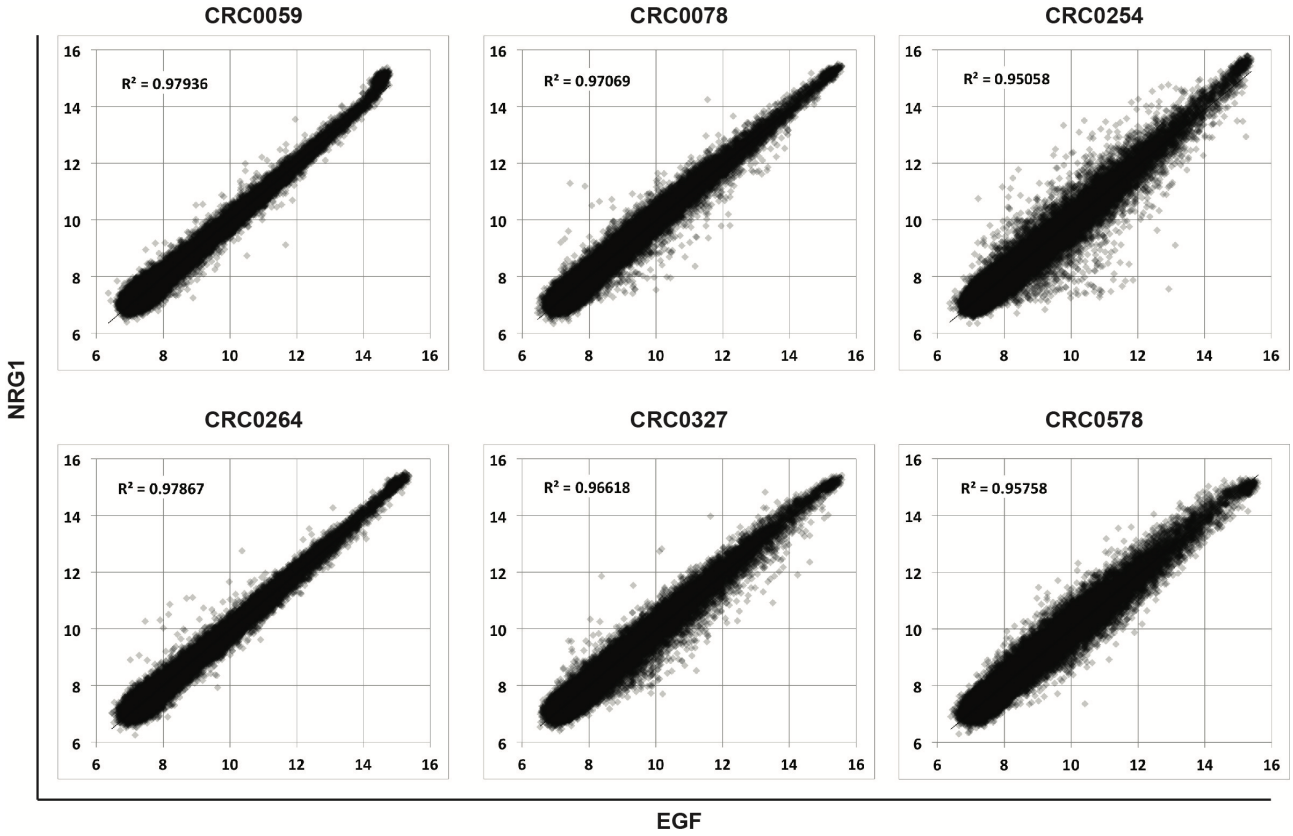

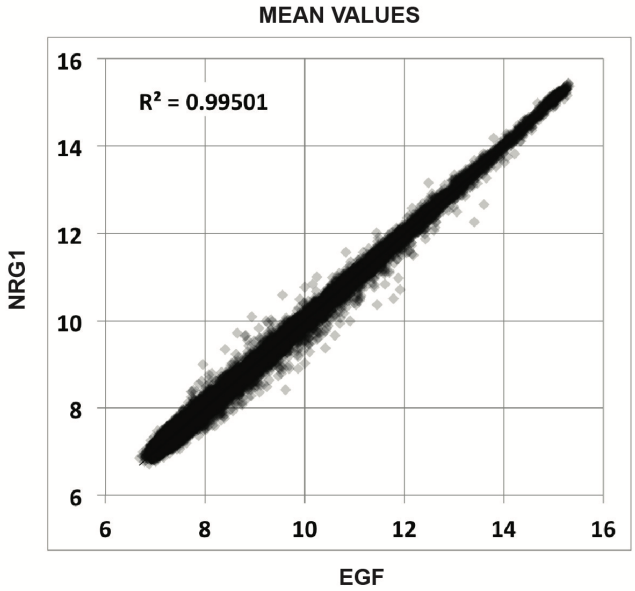

Supplementary Figure 4.

Scatter plots of the Log2 expression values of gene expression profiles of the indicated xenospheres long-term cultured either in standard stem-cell medium containing EGF-bFGF or in a modified medium containing NRG1-bFGF (GEO accession number GSE101792). R^2 values are indicated in the graphs.

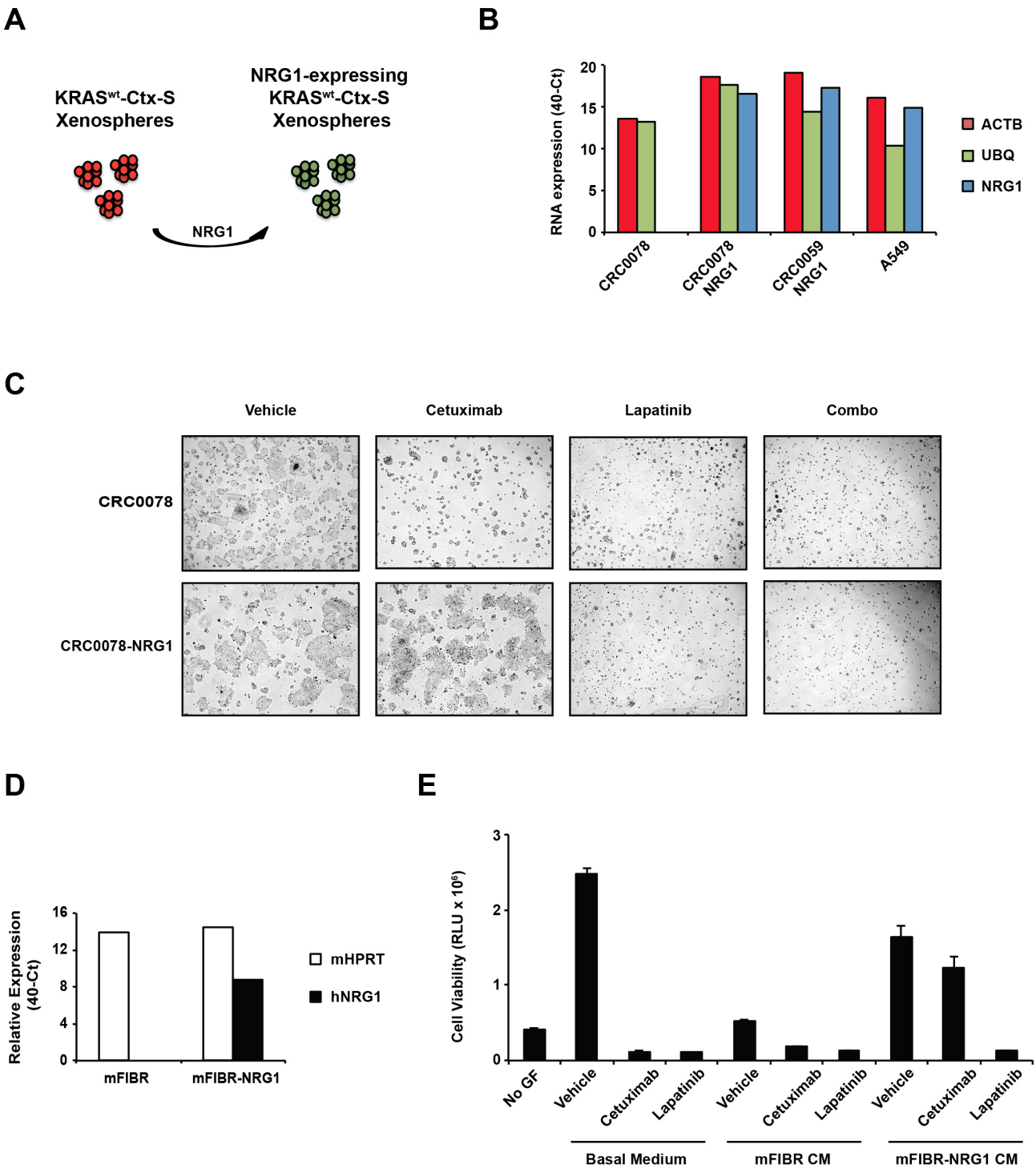

Supplementary Figure 5.

A, Schematic representation of the induction of an NRG1 autocrine loop in KRAS^{wt} xenospheres. **B**, qPCR showing the expression of NRG1 in parental (CRC0078) and transduced (CRC0078-NRG1 and CRC0059-NRG1) xenospheres. A549 cells were used as a positive control for NRG1 expression. Actin B (ACTB) and ubiquitin (UBQ) were used as housekeeper genes. **C**, Micrographs of phase contrast images of parental and NRG1-expressing CRC0078 xenospheres kept in standard

cell culture conditions (i.e. with 10% serum and adhesive plastic) for 1 week, and treated either with vehicle, cetuximab (10 μg/ml), lapatinib (0,5 μM), or their combination (Combo). 20X magnification. **D**, qPCR showing the expression of NRG1 in parental (mFIBR) and NRG1-expressing mouse fibroblasts. mHPRT was used as housekeeper gene. **E**, Cell viability assay of CRC0078 xenospheres kept for 4 days in stem-cell medium without any growth factor (No GF) or with 0,4 ng/ml EGF (Basal Medium), or conditioned medium of parental and NRG1-expressing murine fibroblast (mFIBR-CM and mFIBR-NRG1-CM, respectively), and treated with vehicle, cetuximab (10 μg/ml), or lapatinib (0,5 μM). Columns represent raw RLU data ± s.e.m (n = 3).

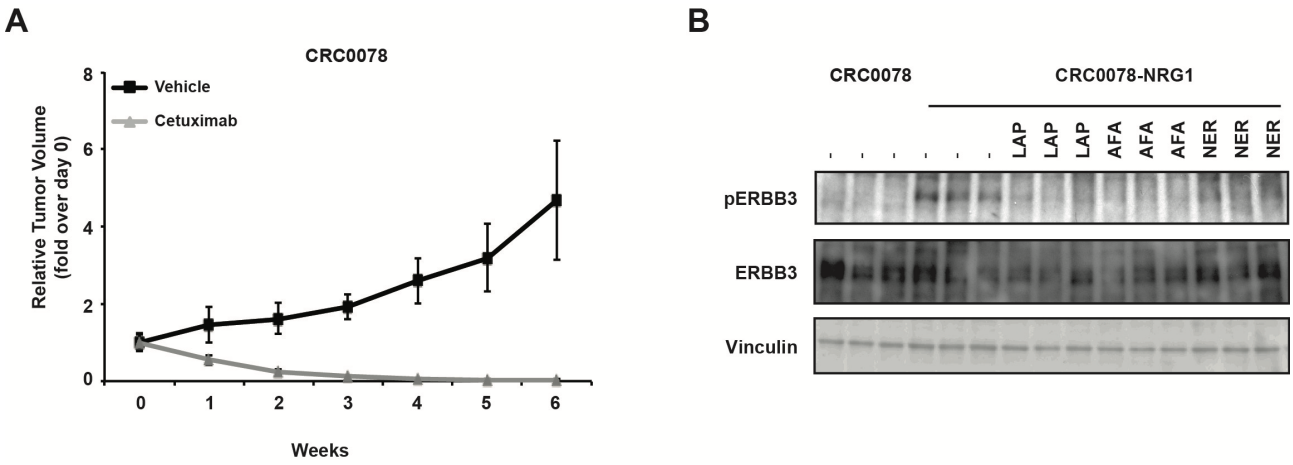

Supplementary Figure 6.

A, Tumor growth curves of CRC0078 spheropatients treated as indicated. Graphs represent tumor volume increase vs. day 0 ± s.e.m. (n = 6/group). **B**, Western Blot analysis of total protein extracts from CRC0078 and CRC0078-NRG1 spheropatients treated for 3 weeks (as in Figure 6F).